The Porphyrinogen−Porphodimethene Relationship Leading to Novel Synthetic Methodologies Focused on the Modification and Functionalization of the Porphyrinogen and Porphodimethene Skeletons

Lucia Bonomo,[†] Euro Solari,[†] Rosario Scopelliti,[†] Carlo Floriani,*[,†] and Nazzareno Re[‡]

Contribution from the Institut de Chimie Minérale et Analytique, BCH, Université de Lausanne, CH-1015 Lausanne, Switzerland, and Facoltà di Farmacia, Università degli Studi "G. D'Annunzio", I-66100 Chieti, Italy

Received January 24, 2000

Abstract: The general synthetic methods presented in this paper make available, on a preparative scale, unprecedented porphyrinogen-derived skeletons, including their functionalization at the meso positions. The stepwise dealkylation of *meso*-octaalkylporphyrinogen $R_8N_4H_4$ [R = Et, **1**; R = Bu^n, **2**] was chemically, mechanistically, and structurally followed until the formation of porphomethene and porphodimethene derivatives **5**−**13**, obtained with a sequential use of $SnCl_4$. In particular, the porphodimethene derivative [$(Et_6N_4)SnCl_2$], **9**, was reductively transmetalated using Li metal to $Et_6N_4Li_2$, **14**, subsequently hydrolyzed to $Et_6N_4H_2$, **15**. The porphodimethene−nickel complex [(Et_6N_4)Ni], **16**, was used for studying the reactivity and the ligand modification of the porphodimethene skeleton. The reactivity of **16** toward nucleophiles led to otherwise inaccessible meso-substituted-meso-functionalized porphyrinogens [$(Et_6N_4R_2)NiLi_2$], [R = H, **18**; R = Bu^n, **19**; R = CH_2CN, **20**], thus exemplifying a general methodology to meso-functionalized porphyrinogens. In addition, when $[NMe_2]^-$ was used as the nucleophile, **16** was converted into mono- and bis-vinylideneporphyrinogen derivatives [$\{Et_4(=CHMe)N_4\}$NiLi], **21**, and [$\{Et_5(=CHMe)_2N_4\}NiLi_2$], **22**, through the intermediacy of *meso*-(dimethylamino)-porphyrinogens undergoing an α-H elimination from the meso positions. Such intermediates were isolated and characterized in the stepwise reaction of **14** with $LiNMe_2$ leading to [$\{Et_6(NMe_2)_2N_4\}Li_4$], **23**, and [$\{Et_5(NMe_2)(=CHMe)N_4\}Li_4$], **25**. Both compounds, as a function of the reaction solvent, undergo the thermal elimination of $HNMe_2$ with the formation of [$\{Et_4(=CHMe)_2N_4\}Li_4$], **24**, which is then protonated to [$\{Et_4(=CHMe)_2N_4\}H_4$], **27**. Transmetalation from **23** to **24** can be used as the methodology for the synthesis of a remarkable variety of meso-substituted and functionalized porphyrinogen complexes. The deprotonation of **16** is reversible, therefore **22** and **23** can be protonated back to their starting materials. We took advantage of the nucleophilicity of the vinylidene carbon in **21** and **22** for establishing a general synthetic method to produce meso-functionalized porphodimethenes. This approach was exemplified with the alkylation and the benzoylation of **22** and **21** leading to [$\{Et_4Pr^i_2N_4\}$Ni], **28**, [$Et_4\{CH(Me)(PhCO)\}_2N_4$Ni], **29**, and [$Et_5\{CH(Me)(PhCO)\}N_4$Ni], **30**, respectively. Complex **21** displays a bifunctional behavior, as shown by the formation of **30**, whereas in the reaction with LiBu, led to [$\{Et_5(Bu^n)(=CHMe)N_4\}NiLi_2$], **31**.

Introduction

Porphyrinogen, namely the *meso*-tetrahydro-tetraalkyl(aryl)-porphyrin, a keystone in the scenario of chemically and biologically relevant molecules, still remains a mysterious molecule due to its instability toward spontaneous autoxidation to porphyrin.[1] The recent modeling studies performed using the much more stable *meso*-octaalkyl derivative[2] disclosed, however, a number of so-far unforeseen but fundamental features of its redox[2b] and acid−base chemistry.[3] This paper deals with the genesis of porphodimethene, the skeleton paving the way from porphyrinogen to porphyrin,[4] and its chemistry, which revealed the interesting relationship with the porphyrinogen skeleton. Chart 1 displays the stepwise oxidation of *meso*-octaalkylporphyrinogen to porphomethene and porphodimethene, which is formally the four-electron oxidized form of porphyrinogen. The novelty in the present synthesis of porphodimethene rests in two major facts: (*i*) its generation from the porphyrinogen skeleton using a metal-assisted transformation; and (*ii*) the large amount of porphodimethene derivatives produced out of this

* To whom correspondence should be addressed.
[†] Université de Lausanne.
[‡] Università degli Studi "G. D'Annunzio".

(1) (a) Lindsey, J. S. In *The Porphyrin Handbook*; Kadish, K. M., Smith, K. M., Guilard, R., Eds.; Academic: Burlington, MA, 1999; Vol. 1, Chapter 2. (b) Kim, J. B.; Adler, A. D.; Longo, F. R. In *The Porphyrins*; Dolphin, D., Ed.; Academic: New York, 1978; Vol. I, Chapter 3. (c) Paine, J. B., III. In *The Porphyrins*; Dolphin, D., Ed.; Academic: New York, 1978; Vol. I, Chapter 4. (d) Scheer, H. In *The Porphyrins*; Dolphin, D., Ed.; Academic: New York, 1978; Vol. II, Chapter 1. (e) Scheer, H.; Inhoffen, H. H. In *The Porphyrins*; Dolphin, D., Ed.; Academic: New York, 1978; Vol. II; Chapter 2. (f) Mauzerall, D. In *The Porphyrins*; Dolphin, D., Ed.; Academic: New York, 1978; Vol. II; Chapter 3. (g) Smith, K. M. *Porphyrins and Metalloporphyrins*; Elsevier: Amsterdam, 1975.

(2) Floriani, C.; Floriani-Moro, R. In *The Porphyrin Handbook*; Kadish, K. M., Smith, K. M., Guilard, R., Eds.; Academic: Burlington, MA; 1999; Vol. 3: (a) Chapter 24 and references therein, (b) Chapter 25 and references therein.

(3) Bonomo, L.; Solari, E.; Floriani, C.; Chiesi-Villa, A.; Rizzoli, C. *J. Am. Chem. Soc.* **1998**, *120*, 12972.

(4) (a) Mauzerall, D.; Granick, S. *J. Biol. Chem.* **1958**, *232*, 1141. (b) Woodward, R. B. *Angew. Chem.* **1960**, *72*, 651. (c) Treibs, A.; Häberle, H. *Justus Liebigs Ann. Chem.* **1968**, *718*, 183. (d) Dolphin, D. *J. Heterocycl. Chem.* **1970**, *7*, 275. (e) Montforts, F.-P.; Gerlach, B.; Höper, F. *Chem. Rev.* **1994**, *94*, 327.

10.1021/ja000253s CCC: $19.00
Published on Web 05/18/2000

Chart 1

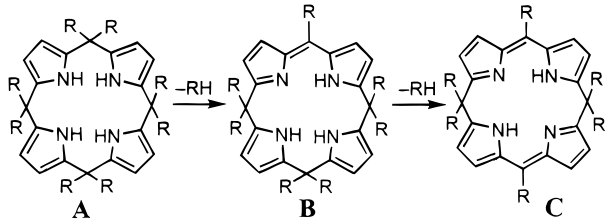

methodology. Two less interesting synthetic approaches have been avoided, namely the reductive alkylation of the porphyrin[5] or the stepwise synthesis from dipyrromethane.[6] None of these synthetic approaches would have even a vague relationship with any natural genesis of the porphodimethene skeleton. In addition, only small amounts of compounds are available from such synthetic routes.[5,6] The reactivity studies carried out on the free or metal-bonded porphodimethenes revealed the access, via the nucleophilic attack to the meso position, to a variety of unprecedented porphyrinogens, including those containing heteroatoms in the meso positions. Particularly relevant, in this context, was the formation of *meso*-bisvinylidene porphyrinogens. The latter allowed the establishment of a quite general synthetic methodology for acceding to functionalizable porphodimethenes. Partial preliminary results have been communicated.[7]

A few of the species reported in this paper have some analogues in the literature, though the later species were generated through convoluted pathways and only in very limited quantities. They appear more like chemical curiosities than starting materials appropriate for synthetic purposes. We took care to uncover not only the porphyrinogen−porphodimethene relationship, but also to establish a synthetic methodology which makes available to the users the skeletons listed in Chart 2 and their derivatives containing functionalities in the meso positions.

Experimental Section

All operations were carried out under an atmosphere of purified nitrogen. All solvents were purified by standard methods and freshly distilled prior to use. NMR spectra were recorded on a 200-AC or DPX-400 Bruker instrument; IR spectra were recorded with a Perkin-Elmer FT 1600 spectrophotometer. GC−MS analyses were carried out using a Hewlett-Packard 5890A GC system. Elemental analyses were performed using an EA 1110 CHN elemental analyzer by CE Instruments. The *meso*-octaalkylporphyrinogens and their lithium derivatives were synthesized according to the literature.[2a]

Synthesis of 5. $SnCl_4(THF)_2$ (28.5 g, 70.4 mmol) was added portionwise to a solution of **3** (60.0 g, 70.4 mmol) in toluene (700 mL). The reaction mixture was refluxed overnight. The undissolved white solid, LiCl, was filtered off and the resulting pink-violet solution was evaporated to dryness. *n*-Hexane (300 mL) was added to the residue to give a pink powder which was collected and dried in vacuo (40.0 g, 71%). Crystals suitable for X-ray diffraction were grown in a mixture of tetrahydrofuran (THF)/*n*-hexane. ^{1}H NMR (C_6D_6, 200 MHz, 298 K, ppm): δ 6.37 (s, 8H, C_4H_2N); 3.13 (m, 8H, THF); 1.96 (q, J = 7.4 Hz, 16H, CH_2); 1.08 (m, 8H, THF); 0.90 (t, J = 7.4 Hz, 24H, CH_3). Anal. Calcd for **5**, $C_{44}H_{64}N_4O_2Sn$: C, 66.08; H, 8.07; N, 7.01. Found: C, 66.12; H, 8.51; N, 7.04.

Chart 2

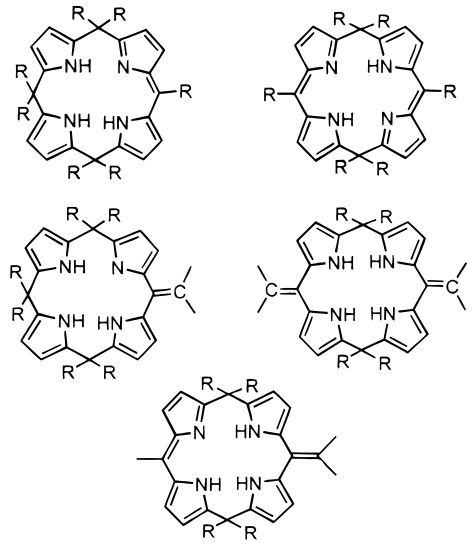

Synthesis of 6. $SnCl_4(THF)_2$ (17.8 g, 44.0 mmol) was slowly added to a solution of **4** (50.2 g, 44.0 mmol) in toluene (700 mL). The reaction mixture was refluxed overnight. The undissolved white solid, LiCl, was filtered off and the resulting violet solution was evaporated to dryness. *n*-Pentane (200 mL) was added to the residue to give a light violet powder which was collected and dried in vacuo (31.0 g, 69%). ^{1}H NMR (C_5D_5N, 200 MHz, 298 K): δ 6.43 (s, 8H, C_4H_2N); 3.67 (m, 8H, THF); 1.66 (t, J = 6.8 Hz, 16H, CH_2); 1.3−0.9 (m, 32H, CH_2); 0.77 (t, J = 7.4 Hz, CH_3 overlapping with m, THF, 32H). Anal. Calcd for **6**, $C_{60}H_{96}N_4O_2Sn$: C, 70.37; H, 9.45; N, 5.47. Found: C, 69.95; H, 9.33; N, 5.12.

Synthesis of 7. A solution of $SnCl_4$ (1.0 g, 3.8 mmol) in toluene (50 mL) was added dropwise at −40 °C to a solution of **5** (12.2 g, 15.2 mmol) in toluene (200 mL). The reaction mixture was warmed to room temperature, stirred overnight, and heated for 2 h at 80 °C to complete the reaction. It was evaporated to dryness and the collected liquid was analyzed with the GC−MS technique. H_2SnEt_2, $HSnEt_3$, and $SnEt_4$ were identified. To the solid residue *n*-hexane (70 mL) was added to give a red powder which was collected and dried in vacuo (9.3 g, 61%). Crystals suitable for X-ray diffraction were grown in toluene. ^{1}H NMR (C_6D_6, 400 MHz, 298 K): δ 7.10 (d, J = 4.4 Hz, 2H, C_4H_2N); 6.43 (d, J = 2.93 Hz, 2H, C_4H_2N); 6.38 (d, J = 4.4 Hz, 2H, C_4H_2N); 6.31 (d, J = 2.93 Hz, 2H, C_4H_2N); 3.63 (m, 4H, THF); 3.15 (q, J = 7.34 Hz, 2H, CH_2); 2.70 (q, J = 7.34 Hz, 2H, CH_2); 2.53 (q, J = 7.34 Hz, 2H, CH_2); 2.24 (dq, J_{gem} = 14.2 Hz, J_{vic} = 7.34 Hz, 2H, CH_2); 2.02 (dq, J_{gem} = 14.2 Hz, J_{vic} = 7.34 Hz, 2H, CH_2); 1.95−1.75 (dq, J_{gem} = 14.2 Hz, J_{vic} = 7.34 Hz, 2H, CH_2 overlapping with dq, J_{gem} = 14.2 Hz, J_{vic} = 7.34 Hz, 2H, CH_2); 1.5 (m, 4H, THF); 1.33 (t, J = 7.34 Hz, 3H, CH_3); 1.30 (t, J = 7.34 Hz, 3H, CH_3); 0.92 (t, J = 7.34 Hz, overlapping with t, J = 7.34 Hz, 9H, CH_3); 0.12 (t, J = 7.34 Hz, 6H, CH_3). Anal. Calcd for **7**, $C_{38}H_{51}ClN_4OSn$: C, 62.18; H, 7.00; N, 7.63. Found: C, 62.12; H, 7.23; N, 7.32.

Synthesis of 8. A solution of $SnCl_4$ (1.9 g, 7.3 mmol) in toluene (50 mL) was added dropwise at −30 °C to a solution of **6** (30.0 g, 29.3 mmol) in toluene (300 mL). The reaction mixture was warmed to room temperature and stirred overnight. To complete the reaction, this dark red solution was heated for 4 h at 80 °C. It was evaporated to dryness and *n*-hexane (100 mL) was added to give a red powder which was collected and dried in vacuo (15.4 g, 56%). ^{1}H NMR (C_5D_5N, 400 MHz, 298 K): δ 7.84 (d, J = 4.4 Hz, 2H, C_4H_2N); 6.99 (d, J = 4.4 Hz, 2H, C_4H_2N); 6.51 (d, J = 2.8 Hz, 2H, C_4H_2N); 6.27 (d, J = 2.8 Hz, 2H, C_4H_2N); 3.63 (m, 4H, THF); 3.35 (t, J = 6.85 Hz, 2H, CH_2); 3.12 (t, J = 6.85 Hz, 2H, CH_2); 2.97 (t, J = 6.85 Hz, 2H, CH_2); 2.6−

(5) (a) Botulinski, A.; Buchler, J. W.; Wicholas, M. *Inorg. Chem.* **1987**, *26*, 1540. (b) Buchler, J. W.; Puppe, L. *Justus Liebigs Ann. Chem.* **1970**, *740*, 142. (c) Buchler, J. W.; Lay, K. L.; Smith, P. D.; Scheidt, W. R.; Ruppzecht, G. A.; Kenny, J. E. *J. Organomet. Chem.* **1976**, *110*, 109. (d) Buchler, J. W.; Dreher, C.; Lay, K. L.; Lee, Y. J. A.; Scheidt, W. R. *Inorg. Chem.* **1983**, *22*, 888. (e) Buchler, J. W.; Lay, K. L.; Lee, Y. J. A.; Scheidt, W. R. *Angew. Chem., Int. Ed. Engl.* **1982**, *21*, 432. (f) Dwyer, P. N.; Buchler, J. W.; Scheidt, W. R. *J. Am. Chem. Soc.* **1974**, *96*, 2789. (g) Mauzerall, D. *J. Am. Chem. Soc.* **1962**, *84*, 2437. (h) Renner, M. W.; Buchler, J. W. *J. Phys. Chem.* **1995**, *99*, 8045. (i) Dwyer, P. N.; Puppe, L.; Buchler, J. W.; Scheidt, W. R. *Inorg. Chem.* **1975**, *i*, 1782. (j) Botulinski, A.; Buchler, J. W.; Lee, Y. J. A.; Scheidt, W. R. *Inorg. Chem.* **1988**, *27*, 927. (k) Botulinski, A.; Buchler, J. W.; Tonn, B.; Wicholas, M. *Inorg. Chem.* **1985**, *24*, 3239.

(6) Bonomo, L.; Solari, E.; Floriani, C. Unpublished work.

(7) (a) Benech, J.-M.; Bonomo, L.; Solari, E.; Scopelliti, R.; Floriani, C. *Angew. Chem., Int. Ed. Engl.* **1999**, *38*, 1957. (b) Bonomo, L.; Solari, E.; Scopelliti, R.; Latronico, M.; Floriani, C. *Chem. Commun.* **1999**, 2227.

2.2 (m, 4H, CH_2); 2.1−1.9 (m, 12H, CH_2); 1.9−1.6 (m, 4H, CH_2); 1.6 (m, 4H, THF); 1.4−1.0 (m, 16H, CH_2); 0.90 (t, $J = 7.3$ Hz, 3H, CH_3); 0.85−0.60 (t, $J = 7.34$ Hz, 3H, CH_3 overlapping with t, $J = 7.34$ Hz, 6H and t, $J = 7.34$ Hz, 3H, CH_3); 0.4 (t, $J = 7.34$ Hz, 6H, CH_3). Anal. Calcd for **8**, $C_{52}H_{79}ClN_4OSn$: C, 67.13; H, 8.56; N, 6.02. Found: C, 67.52; H, 8.62; N, 5.97.

Synthesis of 9. $SnCl_4(THF)_2$ (72.8 g, 0.179 mol) was added to a solution of **5** (47.8 g, 0.06 mol) in toluene (400 mL). The reaction mixture was refluxed overnight and after cooling, a red crystalline solid precipitated. This product was collected, washed by extraction with diethyl ether (500 mL), and then dried in vacuo (21.3 g, 53%). Crystals suitable for X-ray diffraction were grown in toluene. ^{1}H NMR (C_5D_5N, 400 MHz, 298 K): δ 7.73 (d, $J = 4.4$ Hz, 4H, C_4H_2N); 6.83 (d, $J = 4.4$ Hz, 4H, C_4H_2N); 2.98 (q, $J = 7.32$ Hz, 4H, CH_2); 2.29 (q, $J = 7.32$ Hz, 8H, CH_2); 1.25 (t, $J = 7.32$ Hz, 6H, CH_3); 0.93 (t, $J = 7.32$ Hz, 12H, CH_3). Anal. Calcd for **9**, $C_{32}H_{38}Cl_2N_4Sn$: C, 57.51; H, 5.73; N, 8.38. Found: C, 57.41; H, 5.84; N, 7.80.

Synthesis of 10. $SnCl_4(THF)_2$ (71.5 g, 176 mmol) was added to a solution of **6** (60.0 g, 58.6 mmol) in toluene (400 mL). The reaction mixture was refluxed overnight and after cooling, a white solid residue was filtered off. The solution was evaporated to dryness and *n*-hexane (200 mL) was added. The resulting brown solid was collected, dried, and finally it was redissolved in benzene (200 mL).The white undissolved solid was filtered off and the solution was evaporated to dryness. *n*-Pentane (150 mL) was added to give a dark red-violet product which was collected and dried in vacuo (27.1 g, 55%). Suitable crystals for X-ray analysis were obtained from a THF−isooctane solution. ^{1}H NMR (C_5D_5N, 400 MHz, 298 K): δ 7.94 (d, $J = 4.4$ Hz, 4H, C_4H_2N); 7.08 (d, $J = 4.4$ Hz, 4H, C_4H_2N); 3.02 (t, $J = 7.8$ Hz, 4H, CH_2); 2.33 (t, $J = 8.3$ Hz, 8H, CH_2); 1.52 (m, 4H, CH_2); 1.45 (m, 8H, CH_2); 1.15 (m, 4H, CH_2); 1.07 (m, 8H, CH_2); 0.59 (t, $J = 7.34$ Hz, 6H, CH_3); 0.52 (t, $J = 7.34$ Hz, 12H, CH_3). ^{1}H NMR (CD_2Cl_2, 400 MHz, 308 K): δ 7.60 (d, $J = 4.4$ Hz, 4H, C_4H_2N); 6.69 (d, $J = 4.4$ Hz, 4H, C_4H_2N); 3.12 (t, $J = 7.8$ Hz, 4H, CH_2); 2.21 (t, $J = 8.8$ Hz, 8H, CH_2); 1.88 (m, 4H, CH_2); 1.56 (m, 4H, CH_2); 1.22 (m, 8H, CH_2); 1.17 (m, 8H, CH_2); 0.59 (t, $J = 7.34$ Hz, 6H, CH_3); 0.52 (t, $J = 7.34$ Hz, 12H, CH_3). ^{1}H NMR (CD_2Cl_2, 400 MHz, 263 K): δ 7.69 (d, $J = 4.4$ Hz, 4H, C_4H_2N); 7.53 (d, $J = 4.4$ Hz, 4H, C_4H_2N); 6.77 (d, $J = 4.4$ Hz, 4H, C_4H_2N); 6.62 (d, $J = 4.4$ Hz, 4H, C_4H_2N); 3.08 (t, $J = 7.8$ Hz, 4H, CH_2 overlapping with t, $J = 7.8$ Hz, 4H, CH_2); 2.24 (t, $J = 8.8$ Hz, 4H, CH_2); 2.14 (t, $J = 8.8$ Hz, 8H, CH_2 overlapping with m, 4H, CH_2); 1.83 (m, 4H, CH_2); 1.78 (m, 4H, CH_2); 1.51 (m, 4H, CH_2 overlapping with m, 4H, CH_2); 1.30 (m, 4H, CH_2); 1.15 (m, 8H, CH_2); 1.13 (m, 4H, CH_2); 1.07 (m, 8H, CH_2); 0.97 (t, $J = 7.34$ Hz, 6H, CH_3, overlapping m, 4H, CH_2); 0.97 (m, 4H, CH_2); 0.82 (t, $J = 7.34$ Hz, 6H, CH_3); 0.74 (t, $J = 7.34$ Hz, 12H, CH_3 overlapping with t, $J = 7.34$ Hz, 6H, CH_3); 0.70 (t, $J = 7.34$ Hz, 6H, CH_3). Anal. Calcd for **10**, $C_{44}H_{62}N_4SnCl_2$: C, 63.17; H, 7.47; N, 6.70. Found: C, 64.42; H, 6.17; N, 6.78.

Synthesis of 11. $SnCl_4(THF)_2$ (19.2 g, 47.3 mmol) was slowly added to a solution of $[\{(CH_2CH_2)_2\}_4N_4Li_4\ (THF)_2]$ (40.0 g, 47.3 mmol) in toluene (700 mL). The reaction mixture was refluxed overnight. The undissolved white solid, LiCl, was filtered off and the resulting pink solution was evaporated to dryness. *n*-Pentane (200 mL) was added to the residue to give a light pink powder which was collected and dried in vacuo (29.0 g, 77%). ^{1}H NMR (C_6D_6, 400 MHz, 298 K): δ 6.41 (s, 8H, C_4H_2N); 3.54 (m, 8H, THF); 1.85 (m, 16H, CH_2); 1.63 (m, 16H, CH_2); 1.41 (m, THF, 8H). Anal. Calcd for **11**, $C_{60}H_{96}N_4O_2Sn$: C, 66.77; H, 7.13; N, 7.08. Found: C, 66.91; H, 7.31; N, 7.12.

Synthesis of 13. $SnCl_4$ (52.8 mL, 0.17 M in toluene, 8.96 mmol) was added dropwise at −40 °C to a solution of **11** (7.1 g, 8.97 mmol) in toluene (200 mL). The reaction mixture was warmed to room temperature and stirred overnight. A yellow-brown solid precipitated which was collected and dried in vacuo. Elemental analysis was consistent with the adduct **12**. Anal. Calcd for **12**, $C_{40}H_{48}Cl_4N_4OSn_2$: C, 49.02; H, 4.94; N, 5.72. Found: C, 48.74; H, 4.72; N, 5.51. This product was then suspended in toluene (200 mL) and refluxed for 24 h. The reaction mixture became red-violet. A white precipitate was filtered off and the solution was evaporated to dryness. *n*-Hexane (100 mL) was added to give a red powder which was collected and dried in vacuo (5.2 g, 77%). Crystals suitable for X-ray diffraction were grown in a mixture of toluene/*n*-hexane and contained *n*-hexane of crystallization. ^{1}H NMR (C_5D_5N, 400 MHz, 298 K): δ 7.59 (d, $J = 4.4$ Hz, 1H, C_4H_2N); 6.79 (d, $J = 4.4$ Hz, 1H, C_4H_2N); 6.65 (s, 1H, C_4H_2N); 6.31 (d, $J = 2.93$ Hz, 1H, C_4H_2N); 6.30 (d, $J = 2.93$ Hz, 1H, C_4H_2N); 6.20 (d, $J = 2.93$ Hz, 1H, C_4H_2N); 6.19 (d, $J = 2.93$ Hz, 1H, C_4H_2N); 3.63 (m, 4H, THF); 3.2−3.1 (m, 2H, CH_2); 2.78 (m, 2H, CH_2); 2.67 (m, 4H, CH_2); 2.58 (m, 2H, CH_2); 2.48 (m, 2H, CH_2); 2.41 (m, 2H, CH_2); 2.34 (m, 2H, CH_2); 2.24 (m, 2H, CH_2); 1.92 (m, 8H, CH_2); 1.83 (m, 4H, CH_2 overlapping with m, 4H, THF); 1.54 (m, 2H, CH_2). Anal. Calcd for **13**, $C_{40}H_{47}ClN_4OSn$: C, 63.72; H, 6.28; N, 7.43. Found: C, 63.52; H, 6.23; N, 7.32.

Synthesis of 14. Li (0.37 g, 52.8 mmol) and naphthalene (1.0 g, 7.8 mmol) were added under argon to a solution of **9** (8.5 g, 13.2 mmol) in THF (200 mL). The reaction mixture was stirred overnight and the metallic residue was filtered off. The resulting orange solution was evaporated to dryness and benzene (200 mL) was added to remove the undissolved LiCl. The solution was evaporated to dryness and the residue washed with *n*-pentane (100 mL). An orange powder was collected and dried in vacuo (4.2 g, 50%). Crystals suitable for X-ray diffraction were grown in a mixture of THF/*n*-hexane. ^{1}H NMR (C_5D_5N, 400 MHz, 298 K, ppm): δ 7.41 (d, $J = 4.4$ Hz, 4H, C_4H_2N); 6.67 (d, $J = 4.4$ Hz, 4H, C_4H_2N); 3.63 (m, 8H, THF); 3.14 (q, $J = 7.32$ Hz, 4H, CH_2); 2.42 (q, $J = 7.32$ Hz, 8H, CH_2); 1.59 (m, 8H, THF); 1.44 (t, $J = 7.32$ Hz, 6H, CH_3); 1.05 (t, $J = 7.32$ Hz, 12H, CH_3). Anal. Calcd for **14**, $C_{40}H_{54}N_4Li_2O_2$: C, 75.45; H, 8.55; N, 8.76. Found: C, 74.8; H, 8.48; N, 8.60.

Synthesis of 15. Water (100 mL) was added to a solution of **14** (1.0 g, 1.6 mmol) in diethyl ether (100 mL). After 1 h stirring at room temperature, the organic phase was removed and the aqueous phase was washed twice with 100 mL Et_2O. Et_2O was evaporated to dryness and the orange residue dissolved in THF (100 mL). The product was dried by azeotropic distillation, and then the solution was evaporated to dryness. An orange powder was obtained which was collected and dried in vacuo (0.52 g, 68%). Crystals suitable for X-ray diffraction were grown in a mixture of Et_2O/*n*-hexane. ^{1}H NMR (C_6D_6, 400 MHz, 298 K, ppm): δ 14.86 (s, 2H, NH); 6.90 (d, $J = 4.4$ Hz, 4H, C_4H_2N); 6.35 (d, $J = 4.4$ Hz, 4H, C_4H_2N); 2.56 (q, $J = 7.34$ Hz, 4H, CH_2 overlapping with s broad, 4H, CH_2); 2.53 (s broad, 4H, CH_2); 1.01 (t, $J = 7.34$ Hz, 18H, CH_3). ^{1}H NMR (C_7D_8, 400 MHz, 310 K, ppm): δ 14.97 (s, 2H, NH); 7.01 (d, $J = 4.4$ Hz, 4H, C_4H_2N); 6.34 (d, $J = 4.4$ Hz, 4H, C_4H_2N); 2.63 (q, $J = 7.34$ Hz, 4H, CH_2); 2.51 (q, $J = 7.34$ Hz, 8H, CH_2); 1.03 (t, $J = 7.34$ Hz, 6H, CH_3); 0.99 (t, $J = 7.34$ Hz, 12H, CH_3). ^{1}H NMR (C_7D_8, 400 MHz, 263 K, ppm): δ 14.65 (s, 2H, NH); 6.78 (d, $J = 4.4$ Hz, 4H, C_4H_2N); 6.37 (d, $J = 4.4$ Hz, 4H, C_4H_2N); 2.62 (q, $J = 7.34$ Hz, 4H, CH_2); 2.55 (q, $J = 7.34$ Hz, 4H, CH_2); 2.50 (q, $J = 7.34$ Hz, 4H, CH_2); 1.02 (t, $J = 7.34$ Hz, 6H, CH_3); 1.0 (t, $J = 7.34$ Hz, 6H, CH_3); 0.97 (t, $J = 7.34$. Hz, 6H, CH_3). Anal. Calcd for **15**, $C_{32}H_{40}N_4$: C, 79.96; H, 8.39; N, 11.65. Found: C, 79.8; H, 8.03; N, 11.53.

Synthesis of 16. $[NiCl_2(DME)]$ (1.03 g, 4.69 mmol) was added to a solution of **14** (3.04 g, 4.69 mmol) in THF (200 mL). The red solution obtained was stirred overnight at room temperature. The solvent was evaporated and benzene (200 mL) allowed to dissolved the residue. LiCl was removed by filtration. The solution was evaporated to dryness and the residue triturated with *n*-pentane (100 mL) to give a red-violet powder which was collected and dried in vacuo (2.1 g, 76.6%). ^{1}H NMR (C_6D_6, 400 MHz, 298 K, ppm): δ 7.07 (d, $J = 4.4$ Hz, 4H, C_4H_2N); 6.30 (d, $J = 4.4$ Hz, 4H, C_4H_2N); 3.44 (s broad, 4H, CH_2); 2.65 (q, $J = 7.34$ Hz, 4H, CH_2); 1.96 (s broad, 4H, CH_2); 1.07 (m, 18H, CH_3). ^{1}H NMR (C_6D_6, 400 MHz, 318 K, ppm): δ 7.13 (d, $J = 4.4$ Hz, 4H, C_4H_2N); 6.24 (d, $J = 4.4$ Hz, 4H, C_4H_2N); 2.95 (q, $J = 7.34$ Hz, 4H, CH_2); 2.45 (q, $J = 7.34$ Hz, 8H, CH_2); 1.20 (t, $J = 7.34$ Hz, 6H, CH_3); 1.04 (t, $J = 7.34$ Hz, 12H, CH_3). Anal. Calcd for **16**, $C_{32}H_{38}N_4Ni$: C, 71.52; H, 7.13; N, 10.43. Found: C, 71.49; H, 7.15; N, 10.6.

Synthesis of 17. Activated magnesium (0.73 g, 30.0 mmol) was added to **9** (10 g, 15.0 mmol) in THF (300 mL). The red mixture was stirred at room temperature for 24 h until it became violet. The metallic residue was filtered off. The red solution was evaporated to dryness. The residue was dissolved in 150 mL of dichloromethane and the solution was evaporated to dryness. Upon a further addition of

dichloromethane (150 mL), a white solid precipitated which was filtered off. The solution was then evaporated to dryness and *n*-pentane was added to give an orange powder which was collected and dried in vacuo (6.5 g, 67%). Crystals suitable for X-ray diffraction were grown in a mixture of THF/*n*-hexane. ^{1}H NMR (C_5D_5N, 200 MHz, 298 K, ppm): δ 7.61 (d, J = 4.4 Hz, 4H, C_4H_2N); 6.58 (d, J = 4.4 Hz, 4H, C_4H_2N); 3.67 (m, 8H, THF); 3.33 (q, J = 7.4 Hz, 4H, CH_2); 1.98 (q, J = 7.4 Hz, 8H, CH_2); 1.98 (t, J = 7.4 Hz, 6H, CH_3 + m, 8H, THF); 0.18 (t, J = 7.4 Hz, 12H, CH_3). Anal. Calcd for **17**, $C_{40}H_{54}N_4MgO_2$: C, 74.23; H, 8.41; N, 8.66. Found: C, 74.8; H, 8.23; N, 8.53.

Synthesis of 18. $LiHBEt_3$ (7.58 mL, 1.0 M in THF, 7.58 mmol) was added at room temperature to a solution of **16** (2.0 g, 3.79 mmol) in THF (100 mL). The reaction mixture turned immediately violet, was stirred overnight, and then was evaporated to dryness. The pink solid residue was collected with Et_2O (60 mL) and dried in vacuo (2.3 g, 72%). Analysis ^{1}H NMR of reaction mixture and collected product showed that a mixture of syn and anti isomers in a 1:4 ratio was formed. ^{1}H NMR (C_5D_5N, 400 MHz, 298 K, ppm): δ 6.25 (d, J = 2.9 Hz, 8H, C_4H_2N); 6.24 (d, J = 2.9 Hz, 4H, C_4H_2N); 6.23 (d, J = 2.9 Hz, 8H, C_4H_2N); 6.21 (d, J = 2.9 Hz, C_4H_2N overlapping with d, J = 2.9 Hz, C_4H_2N, 12H); 6.19 (d, J = 2.9 Hz, 8H, C_4H_2N); 4.94 (t, J = 5.87 Hz, 4H, H_{endo}); 4.59 (t, J = 5.87 Hz, 2H, H_{endo}); 4.09 (t, J = 7.34 Hz, 4H, H_{exo}); 3.69 (dq, J_{gem} = 14.2 Hz, J_{vic} = 7.34 Hz, 8H, CH_2); 3.60 (dq, J_{gem} = 14.2 Hz, J_{vic} = 7.34 Hz, 8H, CH_2 overlapping with m, 80H, THF and q, J = 7.34 Hz, 4H, CH_2); 3.28 (q, J = 7.34 Hz, 4H, CH_2); 2.95 (m, 8H, CH_2); 2.6−2.45 (m, 28H, CH_2); 1.61 (m, 80H, THF); 1.49 (t, J = 7.34 Hz, 12H, CH_3); 1.47 (t, J = 7.34 Hz, 24H, CH_3 overlapping with t, J = 7.34 Hz, 6H, CH_3); 1.43 (t, J = 7.34 Hz, 6H, CH_3); 1.16 (t, J = 7.34 Hz, 24H, CH_3 overlapping with t, J = 7.34 Hz, 6H, CH_3); 1.10 (t, J = 7.34 Hz, 12H, CH_3). Anal. Calcd for **18**, $C_{48}H_{72}N_4Li_2NiO_4$: C, 68.5; H, 8.62; N, 6.66. Found: C, 68.37; H, 8.53; N, 6.24.

Synthesis of 19. Bu^nLi (4.17 mL, 1.63 M in THF, 6.8 mmol) was added at room temperature to a solution of **16** (1.78 g, 3.4 mmol) in THF (100 mL). A light yellow solution was obtained which was stirred overnight and evaporated to dryness. Et_2O (60 mL) was added to give a yellow solid which was collected and dried in vacuo (2.43 g, 74%). Analysis ^{1}H NMR of reaction mixture and collected product showed that the syn isomer only was formed. ^{1}H NMR (C_5D_5N, 400 MHz, 298 K, ppm): δ 6.25 (d, J = 2.9 Hz, 4H, C_4H_2N); 6.23 (d, J = 2.9 Hz, 4H, C_4H_2N); 3.79 (t, J = 7.8 Hz, 4H, CH_2); 3.66 (m, 16H, THF); 2.57 (q, J = 7.34 Hz, 4H, CH_2); 2.50 (q, J = 7.34 Hz, 4H, CH_2); 1.64 (m, 4H, CH_2 overlapping with m, 16H, THF); 1.50 (t, J = 7.34 Hz, 6H, CH_3 overlapping with m, 4H, CH_2); 1.46 (t, J = 7.34 Hz, 6H, CH_3); 1.21 (m, 4H, CH_2); 1.08 (t, J = 7.34 Hz, 6H, CH_3); 0.61 (t, J = 7.34 Hz, 6H, CH_3). Anal. Calcd for **19**, $C_{56}H_{88}Li_2N_4NiO_4$: C, 70.51; H, 9.30; N, 5.87. Found: C, 70.62; H, 9.27; N, 5.55. The crystals used for the X-ray analysis contain only 3 THF per molecule.

Synthesis of 20. Complex **16** (2.91 g, 5.52 mmol) was added at room temperature to a solution of $LiCH_2CN$ (11.04 mmol) in THF (300 mL). The reaction mixture was stirred for 2 h and then was evaporated to dryness. The pink solid residue was collected with *n*-hexane and dried in vacuo (3.82 g, 75%). Anal. Calcd for **20**, $C_{52}H_{74}Li_2N_6NiO_4$: C, 67.91; H, 8.11; N, 9.14. Found: C, 68.12; H, 8.06; N, 8.99. Analysis ^{1}H NMR of reaction mixture and collected product showed that the syn isomer only was formed. ^{1}H NMR (C_5D_5N, 400 MHz, 298 K, ppm): δ 6.29 (d, J = 2.4 Hz, 4H, C_4H_2N); 6.23 (d, J = 2.4 Hz, 4H, C_4H_2N); 4.63 (s, 4H, CH_2CN); 3.66 (m, 16H, THF); 3.61 (q, J = 7.3 Hz, 4H, CH_2); 2.72 (q, J = 7.3 Hz, 4H, CH_2); 2.45 (q, J = 7.3 Hz, 4H, CH_2); 1.64 (m, 16H, THF); 1.45 (t, J = 7.3 Hz, 6H, CH_3); 1.40 (t, J = 7.3 Hz, 6H, CH_3); 1.07 (t, J = 7.3 Hz, 6H, CH_3). IR (Nujol ν_{max}/cm^{-1}): 2256 (s). The X-ray analysis was performed on the solvated form of **20**, namely $[\{Et_6(CH_2CN)_2N_4\}Ni][Li(DME)_2]_2$ recrystallized slowly at low temperature from 1,2-dimethoxyethane (DME), and it showed to be the anti isomer. After 1 week in deuterated pyridine, all the product was converted in the anti isomer. ^{1}H NMR (C_5D_5N, 400 MHz, 298 K, ppm): δ 6.35 (d, J = 2.9 Hz, 2H, C_4H_2N); 6.27 (d, J = 2.9 Hz, 2H, C_4H_2N); 6.24−6.22 (d, J = 2.9 Hz, 2H, C_4H_2N overlapping with d, J = 2.9 Hz, 2H, C_4H_2N); 4.86 (s, 2H, CH_2CN); 3.75 (dq, J_{gem} = 14.2 Hz, J_{vic} = 7.3 Hz, 2H, CH_2); 3.66 (m, 4H, CH_2 overlapping with m, 16H, THF); 3.61 (dq, J_{gem} = 14.2 Hz, J_{vic} = 7.3 Hz, 2H, CH_2); 3.34 (s, 2H, CH_2CN); 2.72 (q, J = 7.34 Hz, 2H, CH_2); 2.45 (q, J = 7.34 Hz, 4H, CH_2); 1.64 (m, 16H, THF); 1.45 (t, J = 7.34 Hz, 3H, CH_3); 1.40 (t, J = 7.34 Hz, 6H, CH_3); 1.10 (t, J = 7.34 Hz, 6H, CH_3); 1.01 (t, J = 7.34 Hz, 3H, CH_3).

Synthesis of 21. To a solution of **16** (4.0 g, 7.59 mmol) in THF (200 mL) a solution of $LiNMe_2$ (0.39 g, 7.59 mmol) in THF (100 mL) was dropwise added at T = 0 °C. The reaction mixture was warmed to room temperature and stirred for 2 h. The solution was evaporated to dryness. The red solid was collected with *n*-hexane (100 mL) and dried in vacuo (4.28 g, 82%). ^{1}H NMR (C_5D_5N, 400 MHz, 298 K, ppm): δ 7.09 (d, J = 4.4 Hz, 1H, C_4H_2N); 7.07 (d, J = 4.4 Hz, 1H, C_4H_2N); 6.57 (d, J = 2.93 Hz, 1H, C_4H_2N); 6.54 (d, J = 2.93 Hz, 1H, C_4H_2N); 6.41 (d, J = 4.4 Hz, 1H, C_4H_2N); 6.38 (d, J = 2.93 Hz, 1H, C_4H_2N overlapping with d, J = 4.4 Hz, 1H, C_4H_2N); 6.28 (d, J = 2.93 Hz, 1H, C_4H_2N); 6.03 (q, J = 6.85 Hz, 1H, CH); 3.86 (m, 8H, THF); 2.7 (q, J = 7.3 Hz, 2H, CH_2); 2.32−2.28 (m, 8H, CH_2); 2.14 (d, J = 6.85 Hz, 3H, CH_3); 1.61 (m, 8H, THF); 1.30 (t, J = 7.34 Hz, 3H, CH_3); 1.28 (t, J = 7.34 Hz, 3H, CH_3); 1.18 (t, J = 7.34 Hz, 3H, CH_3); 1.10 (t, J = 7.34 Hz, 3H, CH_3); 1.07 (t, J = 7.34 Hz, 3H, CH_3). Anal. Calcd for **21**, $C_{40}H_{53}LiN_4NiO_2$: C, 69.88; H, 7.77; N, 8.15. Found: C, 69.93; H, 8.12; N, 7.97. Reprotonation of **21** with 1 eq of PyHCl in toluene at room temperature gave **16**.

Synthesis of 22. Method A. $LiNMe_2$ (0.74 g, 14.4 mmol) was added in one portion at room temperature to a stirred solution of **16** (3.8 g, 7.22 mmol) in THF (250 mL). The reaction was monitored by NMR and the mixture was stirred until the product **21** was entirely converted ($\approx$ 60 h). The solution was evaporated to dryness. The violet solid was collected with *n*-hexane (100 mL) and dried in vacuo (4.28 g, 71%). Crystals suitable for X-ray diffraction were grown in DME and the X-ray analysis was carried out on the solvated form $[\{Et_4(=CHMe)_2\}Ni][Li(DME)_3]_2$. ^{1}H NMR for the two isomers of **22** (C_5D_5N, 400 MHz, 298 K, ppm): δ 6.55 (m, 8H, C_4H_2N); 6.39 (d, J = 3.2 Hz, 2H, C_4H_2N); 6.38 (d, J = 3.2 Hz, 2H, C_4H_2N); 6.26 (d, J = 2.8 Hz, 2H, C_4H_2N); 6.25 (d, J = 2.8 Hz, 2H, C_4H_2N); 5.87 (q, J = 6.85 Hz, 2H, CH); 5.86 (q, J = 6.85 Hz, 2H, CH); 4.25−3.75 (m, 8H, CH_2); 3.58 (m, 32H, THF); 2.5 (m, 8H, CH_2); 2.18 (d, J = 6.85 Hz, 6H, CH_3 overlapping with d, J = 6.85 Hz, 6H, CH_3); 1.68 (m, 32H, THF); 1.5 (m, 12H, CH_3); 1.19 (t, J = 7.6 Hz, 12H, CH_3). Anal. Calcd for **22**, $C_{48}H_{68}Li_2N_4NiO_4$: C, 68.8; H, 8.18; N, 6.69. Found: C, 68.54; H, 8.02; N, 6.83. Reprotonation of **22** with 1 eq of PyHCl in toluene at room temperature gave **21**. Reprotonation of **22** with 2 eq of PyHCl in toluene at room temperature gave **16**.

Synthesis of 22. Method B. $LiNMe_2$ (0.33 g, 6.54 mmol) was added in one portion at room temperature to a stirred solution of **21** (4.5 g, 6.54 mmol) in THF (250 mL). ^{1}H NMR spectrum of reaction mixture showed the meso-vinylidene-dimethylamino derivative to be present. ^{1}H NMR (C_5D_5N, 400 MHz, 298 K, ppm): δ 6.35 (d, J = 3.4 Hz, 1H, C_4H_2N); 6.34 (d, J = 2.9 Hz, 1H, C_4H_2N); 6.32 (d, J = 2.9 Hz, 1H, C_4H_2N); 6.31 (d, J = 2.9 Hz, 1H, C_4H_2N); 6.29 (d, J = 3.4 Hz, 1H, C_4H_2N); 6.27 (d, J = 3.4 Hz, 1H, C_4H_2N); 6.25 (d, J = 3.4 Hz, 1H, C_4H_2N); 6.11 (d, J = 2.9 Hz, 1H, C_4H_2N); 5.34 (q, J = 7.3 Hz, 1H, CH); 4.1 (dq, J_{gem} = 14.2 Hz, J_{vic} = 7.3 Hz, 1H, CH_2); 3.9 (dq, J_{gem} = 14.2 Hz, J_{vic} = 7.3 Hz, 1H, CH_2); 3.66 (m, 8H, THF); 3.41 (dq, J_{gem} = 14.2 Hz, J_{vic} = 7.3 Hz, 1H, CH_2); 3.33 (dq, J_{gem} = 14.2 Hz, J_{vic} = 7.3 Hz, 1H, CH_2); 2.5 (m, 4H, CH_2); 2.31 (q, J = 7.3 Hz, 2H, CH_2); 2.28 (s broad, 6H, $N(CH_3)_2$); 1.75 (d, J = 7.3 Hz, 3H, CH_3); 1.65 (m, 8H, THF); 1.41 (t, J = 7.3 Hz, 6H, CH_3); 1.2 (t, J = 7.3 Hz, 3H, CH_3); 1.1 (t, J = 7.3 Hz, 3H, CH_3); 1.05 (t, J = 7.3 Hz, 3H, CH_3). The reaction mixture was stirred for 60 h until only **22** was present. The solution was then evaporated to dryness and the violet solid was collected with *n*-hexane (100 mL) and dried in vacuo (4.34 g, 79%). Anal. Calcd for **22**, $C_{48}H_{68}Li_2N_4NiO_4$: C, 68.8; H, 8.18; N, 6.69. Found: C, 69.12; H, 8.32; N, 6.45.

Synthesis of 23. A solution of $LiNMe_2$ (0.32 g, 6.28 mmol) in THF (50 mL) was added dropwise at room temperature to a solution of **14** (2.0 g, 3.14 mmol) in THF (100 mL). The reaction mixture was stirred for 2 h and then was evaporated to dryness. The solid residue was triturated with *n*-hexane to give a light pink powder which was collected and dried in vacuo (2.03 g, 73%). Crystals suitable for X-ray diffraction were grown in a mixture of THF/*n*-hexane. ^{1}H NMR (C_5D_5N, 400 MHz, 298 K, ppm): δ 6.46 (d, J = 2.4 Hz, 4H, C_4H_2N); 6.27 (d, J = 2.4 Hz,

4H, C_4H_2N); 3.70 (m, 16H, THF); 3.25 (q, $J = 7.3$ Hz, 4H, CH_2); 2.99 (q, $J = 7.3$ Hz, 4H, CH_2); 2.17 (q, $J = 7.3$ Hz, 4H, CH_2); 1.93 (s, 12H, CH_3); 1.62 (m, 16H, THF overlapping with t, $J = 7.3$ Hz, 6H, CH_3); 1.05 (t, $J = 7.3$ Hz, 6H, CH_3); 0.83 (t, $J = 7.3$ Hz, 6H, CH_3). Anal. Calcd for **23**, $C_{52}H_{82}Li_4N_6O_4$: C, 70.73; H, 9.36; N, 9.52. Found: C, 70.62; H, 9.17; N, 9.35. Hydrolysis gave **15**.

Synthesis of 24. $LiNMe_2$ (0.63 g, 12.3 mmol) was added at room temperature to a solution of **14** (3.93 g, 6.15 mmol) in benzene (300 mL). After 1 h, ^{1}H NMR showed that **14** was entirely converted into **23**. The reaction mixture was then refluxed for 12 h and was then evaporated to dryness. The light yellow solid residue was collected with *n*-pentane (60 mL) and dried in vacuo (2.8 g, 70%). Anal. Calcd for **24**, $C_{40}H_{52}Li_4N_4O_2$: C, 74.07; H, 8.08; N, 8.64. Found: C, 74.33; H, 8.13; N, 8.45. ^{1}H NMR for the two isomers of **24** (C_5D_5N, 400 MHz, 298 K, ppm): δ 6.91 (d, $J = 2.45$ Hz, 2H, C_4H_2N); 6.86 (d, $J = 2.45$ Hz, 2H, C_4H_2N); 6.74 (d, $J = 2.45$ Hz, 2H, C_4H_2N); 6.69 (d, $J = 2.45$ Hz, 2H, C_4H_2N); 6.47 (d, $J = 2.45$ Hz, 2H, C_4H_2N overlapping with d, $J = 2.4$ Hz, 2H, C_4H_2N); 6.36 (d, $J = 2.45$ Hz, 2H, C_4H_2N overlapping with d, $J = 2.4$ Hz, 2H, C_4H_2N); 5.95 (q, $J = 6.85$ Hz, 2H, CH); 5.88 (q, $J = 6.85$ Hz, 2H, CH); 3.70 (m, 16H, THF); 2.4−2.2 (m, 16H, CH_2); 2.15 (d, $J = 6.85$ Hz, 6H, CH_3 overlapping with d, $J = 6.85$ Hz, 6H, CH_3); 1.62 (m, 16H, THF); 1.00 (m, 24H, CH_3). Anal. Calcd for **23**, $C_{52}H_{82}Li_4N_6O_4$: C, 70.73; H, 9.36; N, 9.52. Found: C, 70.62; H, 9.17; N, 9.35. The X-ray analysis was performed on the polymeric form, $[Et_4(=CHMe)_2N_4Li_4(dioxane)_{3.5}]_n$·dioxane·$C_6H_6$, obtained from dioxane/$C_6H_6$.

Synthesis of 25. Method A. $LiNMe_2$ (0.21 g, 4.12 mmol) was added at room temperature to a solution of **14** (1.31 g, 2.06 mmol) in THF (150 mL). After 1 h, ^{1}H NMR showed that **14** was entirely converted into **23**. The reaction mixture was then refluxed for 12 h and evaporated to dryness. The solid residue was dissolved in *n*-pentane (100 mL) and DME was added dropwise until a yellow microcrystalline solid precipitated. The product was then collected and dried in vacuo (2.0 g, 60%). Crystals suitable for X-ray diffraction were obtained in a mixture of DME/*n*-heptane and have a different solvation, namely $[Et_5(NMe_2)(=CHMe)N_4Li_4(DME)_3]$. ^{1}H NMR ($C_5D_5N$, 400 MHz, 298 K, ppm): δ 6.54 (d, $J = 2.9$ Hz, 1H, C_4H_2N); 6.52 (d, $J = 2.9$ Hz, 1H, C_4H_2N); 6.45 (m, 3H, C_4H_2N); 6.42 (d, $J = 2.9$ Hz, 1H, C_4H_2N); 6.39 (d, $J = 2.9$ Hz, 1H, C_4H_2N); 6.30 (d, $J = 2.9$ Hz, 1H, C_4H_2N); 5.41 (q, $J = 7.3$ Hz, 1H, CH); 3.49 (s, 48H, DME); 3.26 (s, 72H, DME); 2.9−2.68 (m, 2H, CH_2); 2.62 (m, 1H, CH_2); 2.57−2.33 (m, 4H, CH_2); 2.30 (m, 1H, CH_2); 2.26 (q, $J = 7.3$ Hz, 2H, CH_2); 2.02 (s, 3H, CH_3); 1.99 (s, 3H, CH_3); 1.75 (d, $J = 7.3$ Hz, 3H, CH_3); 1.33 (t, $J = 7.3$ Hz, 3H, CH_3 overlapping with t, $J = 7.3$ Hz, 3H, CH_3); 1.19 (t, $J = 7.3$ Hz, 3H, CH_3); 0.77 (t, $J = 7.3$ Hz, 3H, CH_3 overlapping with t, $J = 7.3$ Hz, 3H, CH_3). Anal. Calcd for **25**, $C_{82}H_{163}Li_4N_5O_{24}$: C, 60.39; H, 10.07; N, 4.29. Found: C, 60.32; H, 10.13; N, 4.34. Refluxing in benzene gave **24**.

Synthesis of 25. Method B. $LiNMe_2$ (0.10 g, 1.96 mmol) was added at room temperature to a solution of **26** (1.68 g, 1.96 mmol) in DME (100 mL). After 1 h stirring, ^{1}H NMR showed that **26** was entirely converted into **25**. The reaction mixture was concentrated and *n*-pentane (100 mL) was added to give **25**, which was collected and dried in vacuo (1.82 g, 57%).

Synthesis of 26. $LiNMe_2$ (0.4 g, 7.84 mmol) was added at room temperature to a solution of **5** (2.50 g, 3.92 mmol) in DME (300 mL). After 1 h, ^{1}H NMR showed that **5** was entirely converted into **24**. The reaction mixture was then refluxed for 12 h. A white crystalline solid precipitated and *n*-pentane (200 mL) was added to completely eliminate the excess of $LiNMe_2$ which was filtered off. The solution was then cooled to −20 °C for 12 h and a red crystalline solid precipitated. The product was then collected and dried in vacuo (1.75 g, 52%). Crystals suitable for X-ray diffraction were obtained in a mixture of DME/*n*-pentane. ^{1}H NMR (C_5D_5N, 400 MHz, 298 K, ppm): δ 7.25 (d, $J = 3.2$ Hz, 1H, C_4H_2N); 7.22 (d, $J = 4.0$ Hz, 1H, C_4H_2N); 6.89 (d, $J = 2.8$ Hz, 1H, C_4H_2N); 6.77 (d, $J = 2.8$ Hz, 1H, C_4H_2N); 6.66 (d, $J = 4.0$ Hz, 1H, C_4H_2N); 6.63 (d, $J = 4.0$ Hz, 1H, C_4H_2N); 6.61 (d, $J = 4.0$ Hz, 1H, C_4H_2N); 6.51 (d, $J = 3.2$ Hz, 1H, C_4H_2N); 5.65 (q, $J = 6.85$ Hz, 1H, CH); 3.49 (s, 16H, DME); 3.28 (s, 24H, DME); 2.83 (q, $J = 7.6$ Hz, 2H, CH_2); 2.50 (m, 4H, CH_2); 2.25 (m, 4H, CH_2); 1.95 (d, $J = 6.85$ Hz, 3H, CH_3); 1.23 (t, $J = 7.6$ Hz, 3H, CH_3); 0.85 (t, $J = 7.3$ Hz, 12H, CH_3). Anal. Calcd for **26**, $C_{48}H_{77}Li_3N_4O_8$: C, 67.12; H, 9.03; N, 6.52. Found: C, 67.28; H, 9.15; N, 6.74.

Synthesis of 27. H_2O (1.0 mL) was added to a solution of **24** (5.0, 7.71 mmol) in benzene (100 mL). The reaction mixture was stirred at room temperature for 1 h and the LiOH precipitate was filtered off. The solution was evaporated to dryness and benzene (100 mL) was added again, completely eliminating LiOH. The solvent was evaporated and pentane (50 mL) was added to give a light yellow microcrystalline solid which was collected and dried in vacuo (2.5 g, 67%). Crystals suitable for X-ray diffraction were obtained in *n*-heptane. ^{1}H NMR of the 1:1 mixture of the two isomers (C_6D_6, 400 MHz, 298 K, ppm): δ 9.43 (s broad, 4H, NH); 9.32 (s broad, 2H, NH); 9.17 (s broad, 2H, NH); 6.39 (t, $J = 2.93$ Hz, 2H, C_4H_2N); 6.36 (t, $J = 2.93$ Hz, 2H, C_4H_2N); 6.25 (t, $J = 2.93$ Hz, 2H, C_4H_2N); 6.20 (t, $J = 2.93$ Hz, 2H, C_4H_2N); 6.10 (t, $J = 2.93$ Hz, 2H, C_4H_2N); 6.08−6.05 (t, $J = 2.93$ Hz, 2H, C_4H_2N overlapping with t, $J = 2.93$ Hz, 2H, C_4H_2N); 6.04 (t, $J = 2.93$ Hz, 2H, C_4H_2N); 6.00 (q, $J = 7.34$ Hz, 2H, CH); 5.94 (q, $J = 7.34$ Hz, 2H, CH); 1.87 (d, $J = 7.34$ Hz, 6H, CH_3); 1.82 (d, $J = 7.34$ Hz, 6H, CH_3 overlapping with m, 16H, CH_2); 0.72−0.66 (t, $J = 7.34$ Hz, 12H, CH_3 overlapping t, $J = 7.34$ Hz, 6H, CH_3 and t, $J = 7.34$ Hz, 6H, CH_3). Anal. Calcd for **27**, $C_{32}H_{40}N_4$: C, 79.96; H, 8.39; N, 11.65. Found: C, 79.42; H, 8.02; N, 11.33.

Synthesis of 28. A solution of **22** (1.78 g, 2.32 mmol) in THF (150°mL) was added dropwise at 0 °C to a solution of MeI (0.66 g, 4.65 mmol) in THF (150 mL). The reaction mixture was then warmed to room temperature and stirred overnight. The red-orange solution was evaporated to dryness and benzene (100 mL) was added. The white undissolved solid was filtered off and the solvent evaporated. *n*-Pentane (50 mL) was added to give a red-violet solid which was collected and dried in vacuo (0.9 g, 68%). ^{1}H NMR (C_5D_5N, 400 MHz, 298 K, ppm): δ 7.21 (d, $J = 4.4$ Hz, 4H, C_4H_2N); 6.39 (d, $J = 4.4$ Hz, 4H, C_4H_2N); 3.50 (q, $J = 7.34$ Hz, 2H, CH); 3.42 (q, $J = 7.34$ Hz, 4H, CH_2); 2.08 (q, $J = 7.34$ Hz, 4H, CH_2); 1.33 (d, $J = 7.34$ Hz, 12H, CH_3); 1.05 (t, $J = 7.34$ Hz, 12H, CH_3). Anal. Calcd for **28**, $C_{34}H_{42}N_4Ni$: C, 72.22; H, 7.49; N, 9.91. Found: C, 72.43; H, 7.63; N, 9.34.

Synthesis of 29. PhCOCl (1.68 g, 11.9 mmol) was added at room temperature to a solution of **24** (5.0 g, 5.95 mmol) in THF (300 mL). The reaction mixture was stirred overnight and then evaporated to dryness. Benzene (100 mL) was added and the white undissolved solid was filtered off. The solvent was evaporated and *n*-pentane (50 mL) was added to give a bright red solid which was collected and dried in vacuo (3.7 g, 83%). Anal. Calcd for **29**, $C_{44}H_{46}N_4NiO_2$: C, 74.10; H, 6.22; N, 7.51. Found: C, 74.34; H, 6.42; N, 7.24. ν(C−O) (Nujol), 1684 cm^{-1}. ^{1}H NMR spectrum for the two isomers of **29** (C_5D_5N, 400 MHz, 298 K, ppm): δ 8.33 (d, $J = 7.34$ Hz, 2H, ArH); 8.31 (d, $J = 7.34$ Hz, 2H, ArH); 7.70 (s broad, 4H, C_4H_2N); 7.33 (t, $J = 7.34$ Hz, 2H, ArH); 7.26 (t, $J = 7.34$ Hz, 2H, ArH); 7.12 (m, 4H, ArH); 7.05 (m, 4H, ArH); 6.59 (m, 4H, ArH); 5.14 (q, $J = 6.85$ Hz, 2H, CH); 5.10 (q, $J = 6.85$ Hz, 2H, CH); 3.5−3.2 (s broad, 16H, CH_2); 1.71 (d, $J = 6.85$ Hz, 6H, CH_3); 0.98 (s broad, 12H, CH_3); 0.90 (s broad, 12H, CH_3). ^{1}H NMR (C_5D_5N, 400 MHz, 353 K, ppm): δ 8.22 (d, $J = 7.34$ Hz, 2H, ArH); 8.20 (d, $J = 7.34$ Hz, 2H, ArH); 7.43 (d, $J = 4.4$ Hz, 4H, C_4H_2N); 7.42 (d, $J = 4.4$ Hz, 4H, C_4H_2N); 7.36 (t, $J = 7.34$ Hz, 2H, ArH); 7.30 (t, $J = 7.34$ Hz, 2H, ArH); 7.13 (m, 8H, ArH); 6.42 (d, $J = 4.4$ Hz, 8H, C_4H_2N); 5.04 (m, 4H, CH); 2.75 (q, $J = 7.34$ Hz, 16H, CH_2); 1.77 (d, $J = 6.85$ Hz, 12H, CH_3); 1.07 (t, $J = 7.34$ Hz, 6H, CH_3); 1.00 (t, $J = 7.34$ Hz, 12H, CH_3); 0.93 (t, $J = 7.34$ Hz, 6H, CH_3). Anal. Calcd for **28**, $C_{34}H_{42}N_4Ni$: C, 72.22; H, 7.49; N, 9.91. Found: C, 72.43; H, 7.63; N, 9.34.

Synthesis of 30. PhCOCl (0.55 g, 3.91 mmol) was added at room temperature to a solution of **23** (2.69 g, 3.91 mmol) in THF (100 mL). The reaction mixture was stirred overnight and then evaporated to dryness. Benzene (100 mL) was added and the white undissolved solid was filtered off. The solvent was evaporated and *n*-pentane (50 mL) was added to give a red-orange solid which was collected and dried in vacuo (2.13 g, 85%). Anal. Calcd for **30**, $C_{39}H_{42}N_4NiO$: C, 73.02; H, 6.60; N, 8.73. Found: C, 73.15; H, 6.40; N, 8.47. ^{1}H NMR (C_5D_5N, 400 MHz, 330 K, ppm): 8.17 (d, $J = 7.34$ Hz, 2H, ArH); 7.51 (d, $J = 4.4$ Hz, 2H, C_4H_2N); 7.13 (m, 1H, ArH); 7.06 (d, $J = 4.4$ Hz, 2H, C_4H_2N); 7.01 (m, 2H, ArH); 6.49 (d, $J = 4.4$ Hz, 2H, C_4H_2N); 6.32 (d, $J = 4.4$ Hz, 2H, C_4H_2N); 5.13 (q, $J = 6.85$ Hz, 1H, CH); 2.72 (q, $J =$

7.34 Hz, 2H, CH_2 overlapping with m, 8H, CH_2); 1.78 (d, J = 6.85 Hz, 3H, CH_3); 1.25 (t, J = 7.34 Hz, 3H, CH_3); 1.11 (t, J = 7.34 Hz, 6H, CH_3); 1.06 (t, J = 7.34 Hz, 6H, CH_3).

Synthesis of 31. Bu^nLi (1.0 mL, 1.78 M in *n*-hexane, 1.78 mmol) was added at room temperature to a solution of **21** (1.22 g, 1.78 mmol) in THF (100 mL). A light yellow solution was obtained which was stirred overnight and evaporated to dryness. *N*-pentane (60 mL) was added to give a yellow solid which was collected and dried in vacuo (1.33 g, 83%). ^{1}H NMR (C_5D_5N, 400 MHz, 298 K, ppm): δ 6.57 (d, J = 2.93 Hz, 1H, C_4H_2N); 6.55 (d, J = 2.93 Hz, 1H, C_4H_2N); 6.37 (d, J = 2.93 Hz, 1H, C_4H_2N); 6.36 (d, J = 2.93 Hz, 1H, C_4H_2N); 6.35 (d, J = 2.93 Hz, 1H, C_4H_2N); 6.23 (d, J = 2.93 Hz, 1H, C_4H_2N); 6.22 (d, J = 2.93 Hz, 1H, C_4H_2N); 6.19 (d, J = 2.93 Hz, 1H, C_4H_2N); 6.03 (q, J = 6.85 Hz, 1H, CH_2); 4.25 (dq, J_{gem} = 15.6 Hz, J_{vic} = 7.34 Hz, 1H,CH_2); 4.19 (dq, J_{gem} = 15.6 Hz, J_{vic} = 7.34 Hz, 1H, CH_2); 3.67 (m, CH_2, overlapping with THF, 33H); 3.54 (dq, J_{gem} = 15.6 Hz, J_{vic} = 7.34 Hz, 1H, CH_2); 3.06 (m, 1H, CH_2); 2.9 (m, 1H, CH_2); 2.65−2.50 (m, 4H, CH_2); 2.46 (q, J = 7.34 Hz, 2H, CH_2); 2.34 (d, J = 6.85 Hz, 3H, CH_3); 1.62 (m, 16H, THF); 1.58 (t, J = 7.34 Hz, CH_3 overlapping with m, CH_2, 5H); 1.55 (t, J = 7.34 Hz, 3H, CH_3); 1.39 (t, J = 7.34 Hz, 3H, CH_3); 1.19 (t, J = 7.34 Hz, 3H, CH_3); 1.16 (t, J = 7.34 Hz, 3H, CH_3); 0.7 (m, 2H, CH_2); 0.34 (t, J = 7.34 Hz, 3H, CH_3). Anal. Calcd for **31**, $C_{52}H_{78}Li_2N_4NiO_4$: C, 69.72; H, 8.78; N, 6.25. Found: C, 70.12; H, 8.67; N, 5.95.

X-ray Crystallography for Complexes 14, 15, 16, 20, 22, 23, and 30. Suitable crystals of **14**, **15**, **16**, **20**, **22**, **23**, and **30** were mounted in glass capillaries and sealed under nitrogen. Data concerning crystals, data collection, and structure refinement are listed in Table 1. Data for complexes **16**, **22**, and **30** were collected at 143 K on a mar345 Imaging Plate Detector and reduced with marHKL release 1.9.1.[8] Diffraction data for compounds **14**, **15**, **20**, and **23** were collected at 143 K on a KUMA diffractometer, having a kappa geometry, equipped with a charge-coupled device (CCD) area detector and reduced using CrysAlis RED release 1.6.2.[9] No absorption correction of any kind was applied to any data set. Structure solutions were determined with SIR97.[10] All structures were refined using the full-matrix least-squares on F^2 with all non-H atoms anisotropically defined. Hydrogen atoms were placed in calculated positions using the "riding model" with $U_{iso} = a * U_{eq}$(C) (where a is 1.5 for methyl hydrogens and 1.2 for others, while C is the parent carbon atom). Some particular problems were encountered during the refinement of compound **15** and **22**. In compound **15** the two hydrogens belonging to the nitrogens are disordered over the four nitrogen atoms [the occupancy factor for the hydrogens linked to N2 and N4 is 0.64861, whereas those linked to the other pair of nitrogen (N1 and N3) have an occupancy factor of 0.35139] and the N−H bond distance has been refined (0.96715 Å). In compound **22** a disorder problem, affecting the $CHCH_3$ groups, was solved by finding two different sites (A and B) for the methyl carbon atom (C12) and including them into the structure refinement (occupancy factor for site A = 0.78930). Structure refinement, molecular graphics, and geometrical calculations were carried out on all structures with the SHELXTL software package, release 5.1.[11] Final atomic coordinates, thermal and geometrical parameters, and hydrogen coordinates are listed in the Supporting Information.[12]

Results and Discussion

A. Metal-Assisted Dealkylation of *meso*-Octaalkylporphyrinogen. During the metalation of *meso*-octaalkylporphyrinogens using early transition metals, some degree of dealkylation of the *meso* positions was observed.[13] This kind of metal-

Table 1. Crystal Data and Details of the Structure Determination for **14**, **15**, **16**, **20**, **22**, **23**, and **30**

	14	**15**	**16**	**20**	**22**	**23**	**30**
chemical formula	$C_{40}H_{54}Li_2N_4O_2$	$C_{32}H_{40}N_4$	$C_{32}H_{38}N_4Ni$	$C_{44}H_{62}LiN_6NiO_4{\cdot}C_8H_{20}LiO_4$	$C_{32}H_{36}N_4Ni{\cdot}2C_{12}H_{30}LiO_6$	$C_{52}H_{82}Li_4N_6O4{\cdot}1/2C_6H_{14}$	$C_{39}H_{42}N_4NiO$
formula weight	636.75	480.68	537.37	991.83	1089.96	926.08	641.48
crystal system	monoclinic	triclinic	rhombohedral	triclinic	monoclinic	triclinic	monoclinic
space group	$P2_1/n$	$P-1$	$R-3$	$P-1$	$C2/c$	$P-1$	$P2_1/n$
a (Å)	9.8247(11)	10.9951(19)	35.421(5)	11.9695(17)	12.269(3)	10.9613(13)	16.370(3)
b (Å)	10.9196(12)	11.448(2)	35.421(5)	12.447(2)	19.417(4)	11.6638(14)	12.068(2)
c (Å)	16.940(2)	11.6497(16)	12.136(2)	19.975(3)	26.192(5)	21.6451(13)	17.840(4)
α (deg)	90	65.737(16)	90	91.515(13)	90	86.077(7)	90
β (deg)	90.346(10)	83.522(13)	90	101.210(13)	103.49(3)	86.402(7)	116.82(3)
γ (deg)	90	83.676(15)	120	113.874(16)	90	82.226(10)	90
vol (Å^3)	1817.3(4)	1325.0(4)	13186(4)	2651.1(7)	6067(2)	2731.5(5)	3145.3(11)
Z	2	2	18	2	4	2	4
D_{calc} (g cm^{-3})	1.164	1.205	1.218	1.242	1.193	1.126	1.355
F(000)	688	520	5148	1068	2360	1010	1360
μ (mm^{-1})	0.071	0.071	0.688	0.423	0.379	0.069	0.656
temp (K)	143	143	143	143	143	143	143
wavelength (Å)	0.71073	0.71073	0.71070	0.71073	0.71070	0.71073	0.71070
measured reflections	11469	7700	26963	14170	10943	14426	12695
unique reflections	3418	3892	5157	7324	3664	7520	4187
unique reflections [$I > 2\sigma(I)$]	2616	2997	4197	5655	2120	6481	2453
data/parameters	3418/218	3892/340	5157/335	7324/622	3664/351	7520/622	4187/407
R^a [$I > 2\sigma(I)$]	0.0658	0.0652	0.0580	0.0885	0.0689	0.0997	0.0685
$wR2^a$ (all data)	0.1974	0.1971	0.2050	0.2018	0.2153	0.2774	0.2004
GoF^b 1.098	1.084	1.056	1.124	0.966	1.090	0.943	

^{a} $R = \sum||F_o| - |F_c||/\sum|F_o|$, $wR2 = \{\sum[w(F_o^2 - F_c^2)^2]/\sum[w(F_o^2)^2]\}^{1/2}$. ^{b} GoF = $\{\sum[w(F_o^2 - F_c^2)^2]/(n - p)\}^{1/2}$, where n is the number of data and p is the number of parameters refined.

(8) Otwinowski, Z.; Minor, W. *Methods in Enzymology, Volume 276: Macromolecular Crystallography*; Carter, C. W., Jr., Sweet, R. M., Eds.; Academic: New York, 1997; Part A; pp 307−326.

(9) Kuma Diffraction Instruments GmbH, PSE-EPFL module 3.4, CH-1015, Lausanne, Switzerland, 1999.

(10) Altomare, A.; Burla, M. C.; Camalli, M.; Cascarano, G. L.; Giacovazzo, C.; Guagliardi, A.; Moliterni, A. G. G.; Polidori, G.; Spagna, R. *J. Appl. Crystallogr.* **1999**, *32*, 115.

(11) Bruker AXS, Inc., Madison, WI, 1997.

(12) See paragraph at the end of this paper regarding Supporting Information.

Scheme 1

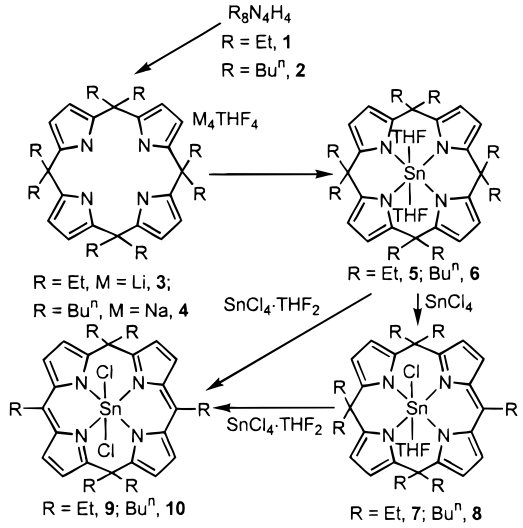

induced dealkylation was hardly understandable and never of a synthetic utility for producing porphomethenes and porphodimethenes. The same synthetic difficulties are encountered using the literature methods, i.e., the reductive alkylation of porphyrins.[5] Therefore, we devised a completely new approach in the field. The synthetic sequence is given in Scheme 1. The metalation of *meso*-octaalkylporphyrinogen $R_8N_4H_4$ [R = Et, Bu^n] was carried out using $SnCl_4$·THF_2. In this context, the use of $SnCl_4$·THF_2[14] is particularly appropriate because it is a solid containing a Lewis acid weaker than $SnCl_4$. The latter property is particularly suitable for carrying the metalation of the porphyrinogen tetraanion. The stannation reaction of **3** and **4** led to **5** and **6**, which contain an octahedral tin(IV) bonded to a porphyrinogen showing a folded and very distorted 1,3 alternate conformation. The reaction of **5** and **6** with $SnCl_4$ in the 4:1 molar ratio led to the formation of the porphomethene−Sn complexes **7** and **8**, which undergo a further *meso*-dealkylation to **9** and **10** when reacted in one-pot reaction with an excess of $SnCl_4$·THF_2. Although the X-ray structure analyses are available on **5**, **7**, **9**, and **10**, they are not reported here, because a number of significant structures of metal complexes issued from the same skeletons are discussed in detail in the following sections. The reaction sequence in Scheme 1 can be formally viewed as the halogenation of the central metal ion and the corresponding elimination of R−$SnCl_3$.

Some significant understanding of the mechanism of such a reaction came from the nature of the meso substituents, the presence of β-hydrogens in the meso substituents being the prerequisite for the easy occurrence of the reaction. Such observations are in agreement with the fact that we were able neither to run the reaction with the *meso*-octamethyl derivative, nor to intercept any R−$SnCl_3$ derivative from the solution. Note that H−$SnCl_3$ was intercepted when the final solution was treated with PhC≡CH or PhC≡CPh, thus obtaining the corresponding vinyl−tin derivatives.[15] We reached the conclusion that the reactions in Scheme 1 proceeds in the case of R = Et or Bu^n with the elimination of H−$SnCl_3$ and the corresponding olefin, namely ethylene or 1-butene. The latter can eventually

Scheme 2

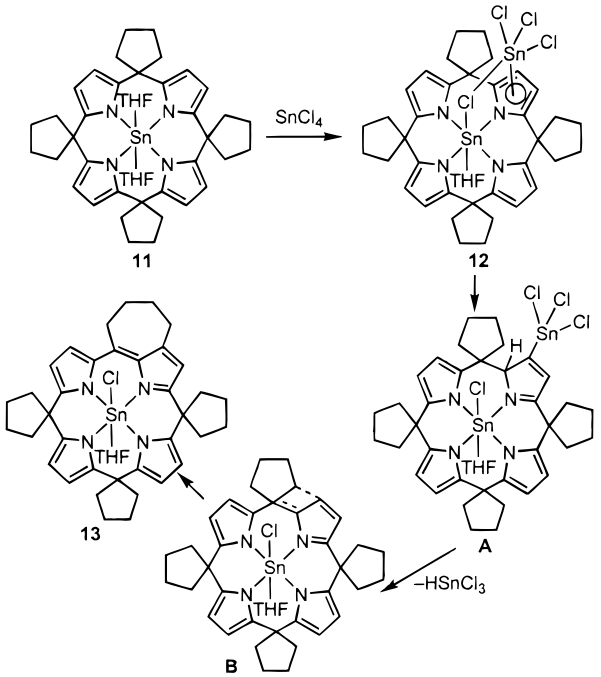

reinsert into the Sn−H bond. To confirm further this hypothesis, the reaction in Scheme 1 was run with the *meso*-tetracyclopentyl derivative, **11**, which might not lose the olefin residue. The reaction led to the formation of **13**, through a plausible mechanism displayed in Scheme 2. We suppose in a preliminary step the binding of $SnCl_4$ by **11** via a bridging chloride and by the use of the electron-rich pyrrolyl anion.[2a] We found spectroscopic and synthetic support for **12**, the later from the reaction of **11** with Ph_3SnCl.[16] We also have a variety of examples where pyrrolyl anions function as η^3 or η^5 binding sites for main group and transition metals.[2a] The conversion of an η^3−η^5 to an η^1 bonding mode and the formation of the σ Sn−C bond (see **A** in Scheme 2) parallels what has been observed for lithium derivatives.[17] The intermediacy of **A** is further supported by the ^{1}H NMR spectrum of the reaction solution, where a singlet appears at 5.83 ppm, typical for the proton in the α position of the pyrrole.[3] The elimination of $HSnCl_3$ from **A** gives rise to a potential free radical coupling with the β position of the pyrrole forming the bicyclic pyrrolyl moiety in **13**. This type of cyclization of the meso substituent, which has some precedent in zirconium−porphyrinogen chemistry with carbon monoxide and isocyanide,[18] has been further confirmed by the use of *meso*-tetracyclohexyl-porphyrinogen−tin in the reaction with $SnCl_4$.[19] The structural support for **13** is given in the Supporting Information.

(13) Solari, E.; Musso, F.; Floriani, C.; Chiesi-Villa, A.; Rizzoli, C. *J. Chem. Soc., Dalton Trans.* **1994**, 2015.

(14) $SnCl_4$·THF_2 can be made simply by addition of a small amount of THF to a toluene solution of $SnCl_4$. Its X-ray structure has been determined.

(15) (a) Pereyre, M.; Quintard, J.-P.; Rahm, A. *Tin in Organic Synthesis*; Butterworth: London, 1987. (b) Davies, A. G. *Organotin Chemistry*; VCH: Weinheim, Germany, 1997; p 88.

(16) Reaction of **11** with Ph_3SnCl: Ph_3SnCl (1.46 g, 3.79 mmol) was added to a solution of **11** (3.0 g, 3.79 mmol) in toluene (100 mL). The reaction mixture was refluxed for 24 h. The solvent was evaporated to dryness and Et_2O (100 mL) was added to give a light orange solid, which was collected and dried in vacuo (2.57 g, 61%). ^{1}H NMR spectrum and elemental analysis revealed a product with Ph_3SnCl, where one of the axial THF at the metal is replaced by the chloride from PH_3SnCl. ^{1}H NMR (C_6D_6, 400 MHz, 298 K, ppm): δ 7.81 (m, 6H, ArH); 7.14 (m, 9H, ArH); 6.33 (s, 8H, C_4H_2N); 3.54 (m, 4H, THF); 2.5 (m, 8H, CH_2); 1.81 (m, 8H, CH_2); 1.77 (m, 8H, CH_2); 1.59 (m, 8H, CH_2); 1.41 (m, 4H, THF). Anal. Calcd for $C_{58}H_{63}ClN_4OSn_2$: C, 63.04; H, 5.75; N, 5.07. Found: C, 62.98; H, 5.81; N, 5.13.

(17) Bonomo, L.; Solari, E.; Latronico, M.; Scopelliti, R.; Floriani, C. *Chem. Eur. J.* **1999**, *5*, 2040.

(18) (a) Jacoby, D.; Isoz, S.; Floriani, C.; Chiesi-Villa, A.; Rizzoli, C. *J. Am. Chem. Soc.* **1995**, *117*, 2805. (b) Floriani, C. *Pure Appl. Chem.* **1996**, *68*, 1.

(19) Bonomo, L.; Solari, E.; Floriani, C. Unpublished work.

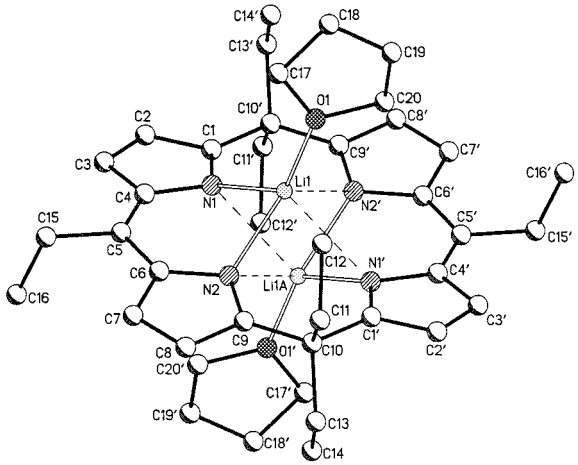

Figure 1. Ball-and-stick representation of complex **14** showing the adopted labeling scheme [hydrogens omitted for clarity]. Prime denotes the following symmetry transformation: $-x, -y, -z$.

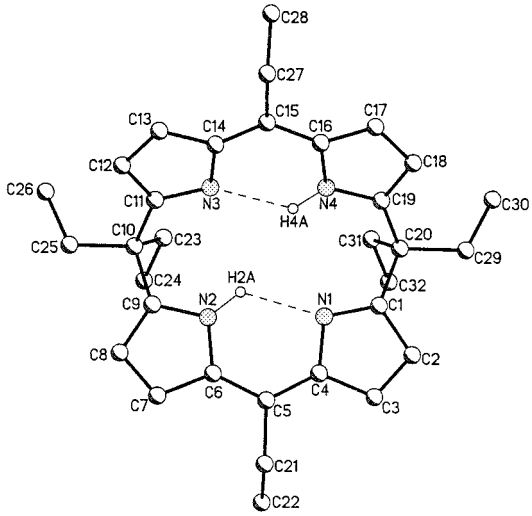

Figure 2. Ball-and-stick representation of compound **15** showing the adopted labeling scheme [only NH hydrogens with the highest occupancy factor are shown].

Scheme 3

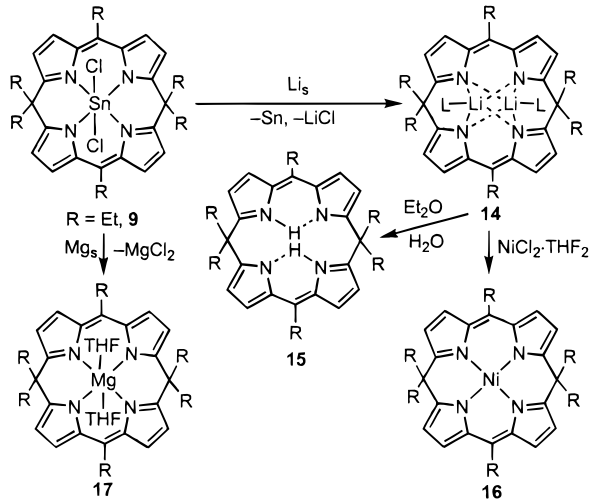

The formation of porphomethenes and porphodimethenes, as reported in Scheme 1, becomes of practical utility under the conditions to find an efficient method for removing the tin ion from the macrocycles. The reductive demetalation of **9** was easily achieved in the reaction with lithium metal in THF. The reaction produces a mirror of tin metal and the lithium porphodimethene. This latter compound is the most appropriate for the entry into the metalated form of porphodimethene, as exemplified by the synthesis of the Ni(II)−porphodimethene complex, **16**, and the protic form, **15** (see Scheme 3). The use of other powerful reducing metals as demetalating agents led instead to the formation of too stable complexes, so that the reaction of **9** with magnesium metal gave the corresponding magnesium−porphodimethene derivative, **17**. The structural analysis of the porphodimethene derivatives in their metalated and nonmetalated form has been examined both in solution and in the solid state by ^{1}H NMR and X-ray analysis, respectively. Structures of **14**, **15**, and **16** are shown in Figures 1−3, respectively, whereas a selection of the conformational and structural parameters is listed in Tables 2 and 3.

The skeleton of the ligand is almost planar for the lithium derivative and saddle-shaped for compounds **15** and **16**. As expected, in **14** the lithium cations show a very pronounced deviation from the N_4 average plane [±1.031(4) Å], whereas in compound **16** the deviation of the nickel atom from the N_4 core is small [0.072(2) Å].

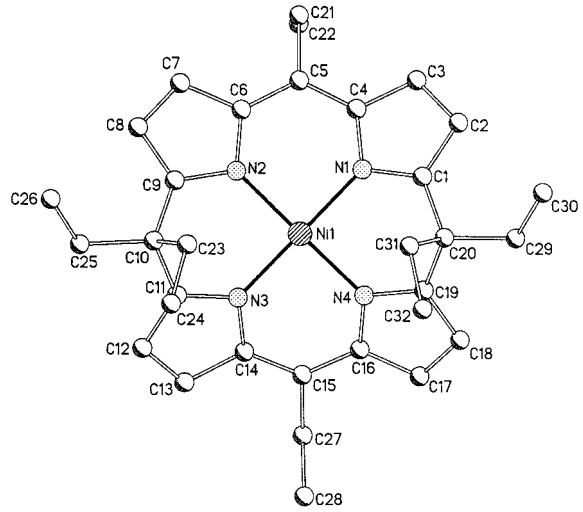

Figure 3. Ball-and-stick representation of complex **16** showing the adopted labeling scheme [hydrogens omitted for clarity].

Significant Ni−H axial interactions, which are probably responsible for minimizing the out-of-plane of Ni, have been observed in the case of **16** between the central metal and the C23 and C31 methylenes [Ni···H, 2.69 and 2.66 Å].[20] The structural parameters in Table 3 support the bonding sequence proposed in Scheme 3. The two lithium cations are squeezed to a very short distance [Li···Li, 2.142(8) Å], because of their binding inside of the N_4 core.[21] The two lithium cations lie on the opposite sides of the N_4 average plane, and they bind two nitrogens at close distances [Li1−N1, 2.113(5); Li1−N2, 2.156(5) Å] and the other two nitrogens at longer distances (Li1−N1′, 2.523(5); Li1−N2′, 2.465(5) Å].

^{1}H NMR spectra of porphomethenes always show two sets of two doublets for the β protons of the pyrroles with one J value in the range 4.0−4.5 and the other J value ≤3. The relative assignment to the different hydrogens (see **D** in Chart 3) was

(20) Similar interactions have been observed in some *meso*-octaalkylporphyrinogens: (a) De Angelis, S.; Solari, E.; Floriani, C.; Chiesi-Villa, A.; Rizzoli, C. *J. Am. Chem. Soc.* **1994**, *116*, 5691 and 5702. (b) Crescenzi, R.; Solari, E.; Floriani, C.; Chiesi-Villa, A.; Rizzoli, C. *J. Am. Chem. Soc.* **1999**, *121*, 1695.

(21) For the binucleating binding ability of *meso*-octaalkylporphyrinogen tetraanion, see: (a) Bonomo, L.; Solari, E.; Floriani, C.; Scopelliti, R. *Angew. Chem., Int. Ed. Engl.* **1999**, *38*, 913.

Table 2. Comparison of Relevant Structural Parameters within the Metal−Ligand or Free Ligand Units

		14	**15**	**16**	**20**	**22**	**23**	**30**
deviations form the N_4 core, Å	N1	0	−0.003(2)	0.009(2)	0.007(2)	−0.006(3)	−0.013(2)	−0.013(2)
	N2	0	0.003(2)	−0.009(2)	−0.007(2)	0.006(3)	0.013(2)	0.013(2)
	N3	0	−0.003(2)	0.009(2)	0.007(2)	−0.006(3)	−0.013(2)	−0.013(3)
	N4	0	0.003(2)	−0.009(2)	−0.007(2)	0.006(3)	0.013(2)	0.013(2)
	M[b]	±1.031(4)	−	0.072(2)	−0.012(2)	0.011(3)	−0.377(8)	−0.046(3)
angle between AB[a], °		12.0(2)	4.6(2)	16.8(1)	38.5(3)	40.5(2)	32.3(2)	30.0(3)
angle between AC[a], °		0	64.7(1)	63.4(2)	65.8(2)	63.0(2)	79.0(2)	58.5(3)
angle between AD[a], °		12.0(2)	61.0(1)	60.8(2)	43.2(3)	44.4(2)	73.7(2)	46.3(3)
angle between BC[a], °		12.0(2)	65.2(1)	57.5(2)	51.1(2)	44.4(2)	68.3(2)	53.6(3)
angle between BD[a], °		0	60.8(1)	62.8(2)	65.2(2)	60.3(2)	76.9(2)	58.1(3)
angle between CD[a], °		12.0(2)	8.8(2)	24.1(2)	48.0(3)	40.5(2)	24.5(2)	26.8(4)
angle between *meso* C sp^2 moieties, °		0	58.1(1)	63.6(2)	−	93.2(3)	−	49.9(3)

[a] A, B, C, and D define the pyrrole rings containing N1, N2, N3, and N4. [b] M = Li in compound **14** and **23**, M = Ni in compound **16**, **20**, **22**, and **30**.

Table 3. Selected Bond (Å) for Compounds **14**, **16**, **20**, **22**, **23**, and **30**

	14	**16**	**20**	**22**	**23**	**30**
M−N1[a]	2.113(5)	1.893(3)	1.858(5)	1.889(4)	2.145(7)	1.889(5)
M−N2[a]	2.156(5)	1.896(3)	1.889(4)	1.884(4)	2.213(7)	1.872(5)
M−N3[a,b]	2.523(5)	1.891(3)	1.871(5)	1.889(5)	2.261(7)	1.879(5)
M−N4[a,b]	2.465(5)	1.893(3)	1.878(4)	1.884(4)	2.195(7)	1.864(5)
C22−N5			1.146(9)			
C30−N6			1.141(8)			
N6−Li1			2.128(12)			
C10−C11				1.316(11)		
Li2−N1					2.025(6)	
Li2−N2					2.077(7)	
Li2−N5					2.103(7)	
Li3−N3					2.136(8)	
Li3−N4					2.061(7)	
Li3−N6					2.172(7)	
Li4-η^5(Pyr)[c]					1.994(9)	
C29−O1						1.236(7)

[a] M is lithium for complex **14** and **23**, whereas it corresponds to nickel for complex **16**, **20**, **22**, and **30**. [b] For complexes **14** and **22**, N3 and N4 correspond to N1′ and N2′ obtained by the following symmetry operations: $-x, -y, -z$ (**14**); $-x, y, -z+1/2$ (**22**). [c] η^5(Pyr) indicates the centroid.

Chart 3

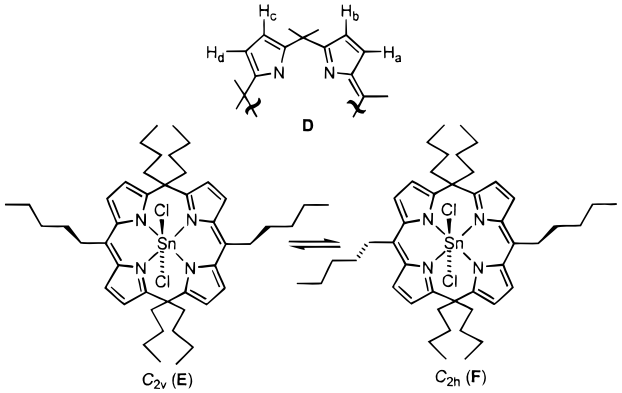

based on coupling constant analysis. The observed multiplicity (d, $J \sim 4.4$ Hz) of the H_a or H_b protons is consistent with an H_a-H_b torsion angle of approximately 2°. The observed multiplicity of H_c or H_d (d, $J \sim 2.9$ Hz,) is in agreement with a minor torsion angle H_c-H_d (1°). ^{1}H NMR spectra of porphodimethenes with a single set of doublets for the β protons of the pyrroles ($J \sim 4.4$ Hz) support what has been mentioned above. Moreover, porphodimethenes generally are expected to have very simple ^{1}H NMR spectra with only two sets of signals for the ethyl groups. For the Ni complex **16** and the nonmetalated derivative **15**, however, this is only true at relatively high temperatures (> 310 K). Note that their ^{1}H NMR spectra recorded in C_7D_8 at a lower temperature (263 K) show three quartets and three triplets of equal intensity for the ethyl groups. This is probably due to the presence of two meso-sp^3 carbons giving rise to a pseudo saddle-shaped conformation with different endo−exo ethyl groups. ^{1}H NMR spectra of the butylporphodimethene−Sn complex, **10**, in deuterated pyridine at room temperature is similar to the corresponding ethyl derivative with a D_{2h} symmetry. When the spectrum is recorded in CD_2Cl_2 at room temperature, all the signals are broad, while at higher temperature (308 K) two doublets for the β protons of the pyrroles and two sets of signals for the butyl groups appear. At lower temperatures (263 K), four doublets for the β protons of the pyrroles and five sets of signals for the butyl group appear, because of the two different conformers shown as **E** and **F** in Chart 3. One is consistent with a C_{2h} symmetry with only two sets of signals for the butyl groups. The other one displays three sets of signals of equal intensity for the butyl groups, in agreement with a C_{2v} symmetry.

B. The Electrophilic Reactivity of Porphodimethenes at the *meso*-Carbon: The Synthesis of Meso-Functionalized Porphyrinogens. The porphodimethene skeleton displays a quite interesting and unprecedented reactivity in its metalated or metal-free form. In both cases the porphodimethene skeleton is quite sensitive to the attack by nucleophiles at the monosubstituted meso-positions.[22] Such a methodology has been recently and successfully used for the meso-functionalization of porphyrins,[22d] though with few nucleophiles. The reactivity of porphodimethene toward nucleophiles, depending on the presence of the metal and the nature of the nucleophile, led to quite interesting synthetic results with the formation of novel forms of porphyrinogen. The electrophilic reactivity of the porphodimethene skeleton was explored using **14** and **16** as starting materials. The reactivity of **16** is displayed in Scheme 4, where three different nucleophiles were used to prove the versatility of such a class of reactions. The reaction of **16** with $LiHBEt_3$ led to a quite unusual *meso*-dehydro-hexaethylporphyrinogen−nickel complex, **18**, which shows a quite unexpected stability. Note that porphyrinogens bearing hydrogens in the meso positions show a high tendency to autooxidize to the corre-

(22) (a) Vicente, M. D. G. H. In *The Porphyrin Handbook*; Kadish, K. M., Smith, K. M., Guilard, R., Eds.; Academic: Burlington, MA, 1999; Vol. 1, Chapter 4. (b) Jacquinot, L. In The *Porphyrin Handbook*; Kadish, K. M., Smith, K. M., Guilard, R., Eds.; Academic: Burlington, MA, 1999; Chapter 5. (c) Fhurhop, J.-H. In *The Porphyrins*, Dolphin, D., Ed.; Academic: New York, 1978; Vol. II, Chapter 5. (d) Kalisch, W. W.; Senge, M. O. *Angew. Chem., Int. Ed. Engl.* **1998**, *37*, 1107 and references therein. (e) Krattinger, B.; Callot, H. J. *Tetrahedron Lett.* **1996**, *37*, 7699. (f) Krattinger, B.; Callot, H. J. *Tetrahedron Lett.* **1998**, *39*, 1165. (g) Krattinger, B.; Callot, H. J. *Chem. Commun.* **1996**, 1341. (h) Sugimoto, H. *J. Chem. Soc., Dalton Trans.* **1982**, 1169. (i) Segawa, H.; Azumi, R.; Shimidzu, T. *J. Am. Chem. Soc.* **1992**, *114*, 7564.

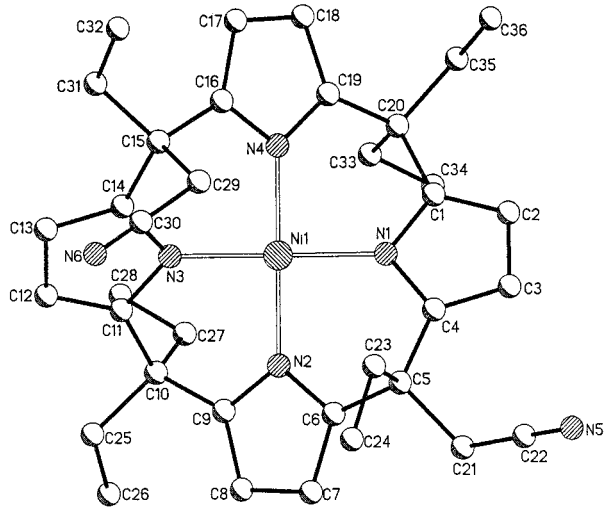

Figure 4. Ball-and-stick representation of the dianion of complex **20** showing the adopted labeling scheme [hydrogens and $Li(DME)_2^+$ cations omitted for clarity].

Scheme 4

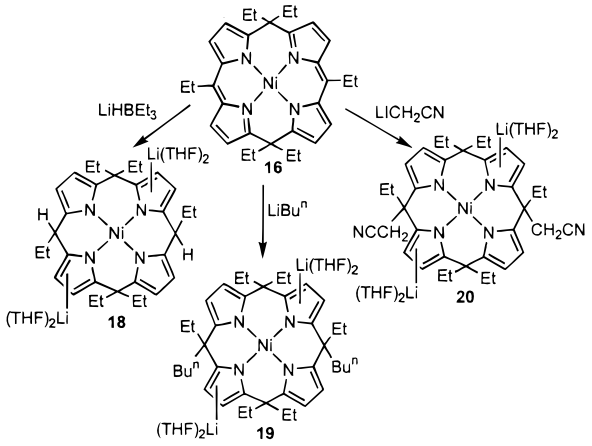

sponding porphodimethene or porphyrin.[1,22] The other two reactions in Scheme 4 were carried out in a similar way using LiBu and $LiCH_2CN$ as nucleophiles. The reactions led to the formation of **19** and **20**, respectively. The $\eta^3-\eta^5$ binding of the lithium countercation is the same as that which we found in several *meso*-octaethylporphyrinogen−metal complexes,[2a] though the ion-pair can be crystallized as the ion-separated form in the presence of strongly binding solvents. This structural feature was further confirmed with X-ray analyses (see below). Two stereoisomers issued from a syn or anti attack at the meso positions are expected in the case of compounds **18**−**20**. Because of such a possibility, the solid state−solution relationship has been carefully analyzed both for the crude and the crystallized compounds. A short summary is given, first, on the common structural features in the solid state of complexes **18**−**20**. They have a very similar structure, which is reported in detail only for the anion in **20** (Figure 4), whereas the structure of **19** is given in the Supporting Information. The X-ray analysis on **20** was performed on the ion-separated form recrystallized from DME. The overall structure of the anion in **20** is quite reminiscent of the *meso*-octaalkylporphyrinogens,[2] albeit the presence of the two CH_2CN functionalities. The conformational parameters in Table 2 are informative about the saddle-shaped conformation of the ligand, with the out-of-plane of the metal distance, −0.012(2) Å, being similar to that in *meso*-octaalkylporphyrinogen−metal derivatives. The two lithium cations are fully solvated by DME, one of them interacting also with the

Chart 4

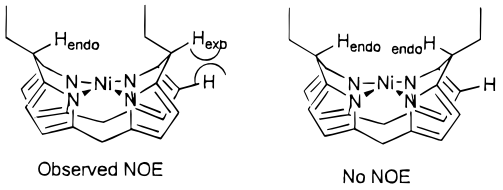

$-CH_2CN$ group [Li1−N6, 2.128(12) Å]. A further common interesting structural feature of **19** (Supporting Information) and **20** is the presence in the axial position of four hydrogens from the *meso*-methylenes in a tetrahedral arrangement around the central metal ion. Three sets of Ni···H interactions can be singled out: (1) Ni1···H (owned by a CH_2CN group), 2.67 Å; (2) Ni1···H (owned by CH_2CH_3 groups), 2.83, 2.84 Å; and (3) Ni···H (owned by a CH_2CH_3 group facing the CH_2CN group which interacts with the lithium and the nickel cations), 3.06 Å.[20] The macrocyclic ligand shows the usual saddle-shaped conformation, with opposite meso sp^3 carbon atoms facing each other. The very distinctive structural feature between **19** and **20** is the difference in the stereoisomer present in the solid state, being the syn for **19** and the anti for **20**. The analysis in solution of **19** and **20** by means of ^1H NMR allowed us to establish the solid state−solution structural relationship. Within this context it should be clarified that the structures drawn in the schemes refer to the solvated forms obtained from the synthesis and they differ slightly from those recrystallized to produce suitable crystals for X-ray analysis. Regardless of the type of solvation, when the ion-pair forms are examined by NMR in solution of strongly coordinating solvents such as Py, they are present in the ion-separated forms, so we refer to the analysis of the anions drawn in the schemes.

The ^1H NMR analysis indicates that the *meso*-dihydrohexaethylporphyrinogen−nickel complex, **18**, was obtained as a mixture of syn and anti isomers in a 1:4 ratio. The relative chemical assignment of the two stereoisomers was based on symmetry considerations. The syn isomer has a C_{2v} symmetry with a set of two doublets for the β-pyrrole protons and one triplet for the meso-protons. The ^1H NMR spectrum of the anti isomer with four doublets for the β pyrrole protons and two triplets for the two different *endo-exo* hydrogens was consistent with a C_s symmetry. The stereochemistry of the two isomers was also confirmed by a two-dimensional (correlation spectroscopy) (COSY), nuclear Overhauser enhancement spectorscopy (NOESY) NMR spectral analysis. For the anti isomer only, large nuclear Overhauser effect (NOE) between the H_{exo} and the β protons was observed (Chart 4). The absence of NOE in the case of the syn isomer suggests that the predominant conformation is that shown in Chart 4 with the hydrogens endo in the meso positions. Examination of the ^1H NMR spectra of **19** and **20** (reaction mixture and isolated product) indicates for both only the syn isomer. For **19** this spectral evidence is in agreement with the solid-state structure, whereas **20** crystallized as the anti isomer. To accommodate this apparent discrepancy between solid state and solution for **20**, it should be assumed that the syn stereoisomer is the kinetic product, whereas the anti isomer is the thermodynamic product. The conversion of the syn into the anti isomer was followed by ^1H NMR spectroscopy. The ^1H NMR spectrum of **20** in deuterated pyridine, carried out immediately after dissolution of the solid, showed the presence of the syn isomer exclusively, whereas 1 day later the appearance of the anti isomer with four doublets for the pyrrole β-protons and two singlets for the two different *endo*−*exo*-CH_2CN groups was observed. The syn → anti

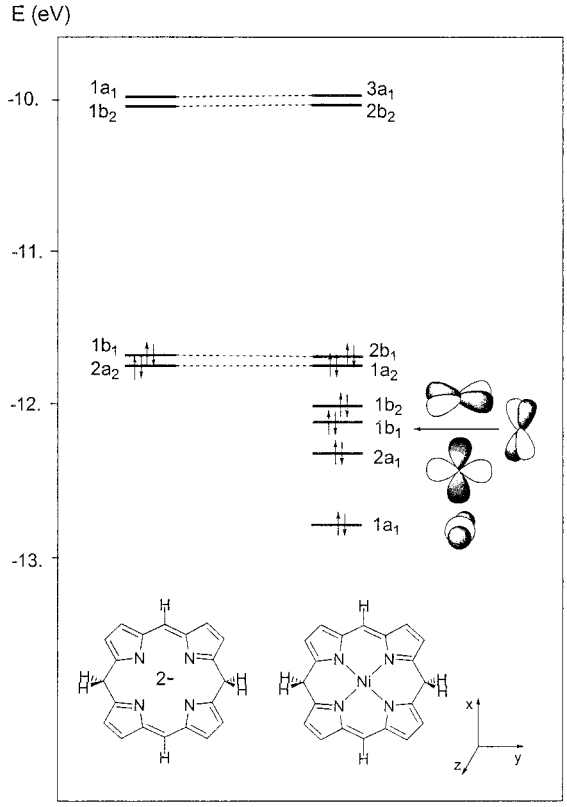

Figure 5. Molecular orbitals of the porphodimethene−nickel complex.

transformation was complete in a week. This type of isomerization is only possible if one admits the reversibility of the nucleophilic attack by the $[CH_2CN]^-$ group at the meso positions of the porphodimethene skeleton, such a reversibility being impossible in the case of alkyl or hydrido nucleophiles. Further examples of reversible nucleophilic reactions at the meso positions of porphodimethenes are reported in the next section.

Note that the three reactions reported in Scheme 4 represent a synthetic methodology to meso-functionalized porphyrinogens, exemplified particularly by **20**, whereas the formation of **18** shows a synthetic access to a potentially unstable porphyrinogen.[1,22] The high and selective reactivity with nucleophiles at the meso positions prompted us to analyze such a behavior with a qualitative theoretical approach.

The molecular orbitals of the nickel−hexaethylporphodimethene fragment are built in a step-by-step approach, using the extended Hückel method.[23] The hexaethylporphodimethene ligand was simplified by replacing the six ethyl groups with hydrogen atoms. We first considered the macrocyclic ligand of C_{2v} symmetry whose molecular orbitals are reported in the first column of Figure 5. We then added the nickel atom and the resulting molecular orbitals (MOs) diagram of this d^8 metal complex is reported in the second column of Figure 5. Upon coordination, the d orbitals mix strongly with the ligand frontier orbitals, but five MOs with large metal d character can be identified. These are the four occupied orbitals $1a_1(d_{z^2})$, $2a_1(d_{x^2-y^2})$, $1b_1(d_{xz})$, and $1b_2(d_{yz})$. The $a_2(d_{xy})$ pointing more closely toward the nitrogen atoms of the ligand, is pushed higher in energy. The two lowest unoccupied (LUMO) (a_1 and b_2) and the two highest occupied (HOMO) (b_1 and a_2) orbitals of the porphodimethene ligand are left essentially unperturbed by the interaction with the metal and remain, respectively, the LUMO and LUMO + 1 and the HOMO and HOMO − 1 for the nickel complex. To understand the factors which determine the observed regioselectivity of the nucleophilic attack on the meso carbon atoms of the macrocyclic ligand, we analyzed both the atomic charges and the frontier orbitals localization. The gross atomic charges derived for the nickel porphodimethene show that the two meso carbons are less positive (+0.07) than the pyrrole β-carbons (+0.32) and the metal (+0.58), thus indicating that the nucleophilic attack is not charge-controlled. On the other hand, the two low-lying empty orbitals $2b_2$ and $3a_1$ are purely ligand-based and mostly localized on the two meso carbons see (Chart 5), thus suggesting that the regioselectivity of the nucleophilic attack on these atoms is controlled by frontier orbitals factors. Note that the $2b_2$ and $3a_1$ are essentially the unaltered LUMO and LUMO + 1 of the free porphodimethene dianion see (Figure 5), and thus determine also the regioselectivity of the nucleophilic attack on the latter species, as exemplified by the synthetic approach in Scheme 6.

Chart 5

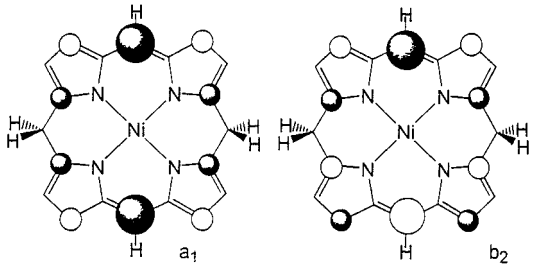

Scheme 5

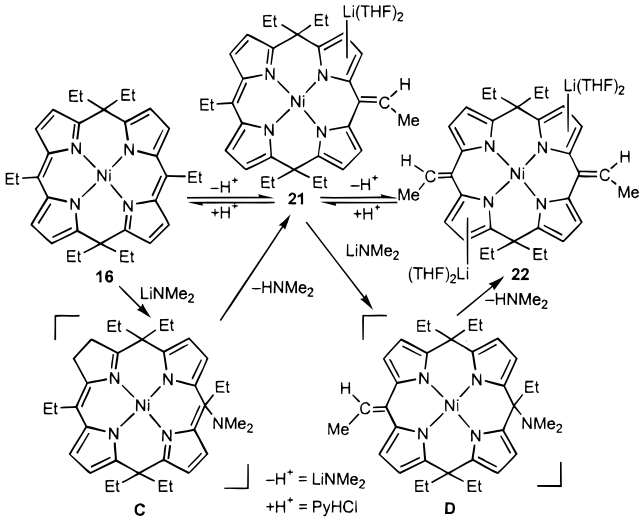

C. Deprotonation of Porphodimethene to bis-Vinylidene-Porphyrinogen. The addition of dimethylamino anions to the meso positions of porphodimethene led, through the intermediacy of **C** and **D** (Scheme 5), to the deprotonation of the ethyl group and the formation of the *meso*-vinylidene−porphyrinogen derivatives **21** and **22**. The proposed pathway involving intermediates **C** and **D** is based on the analogous structure displayed by complexes **18**−**20** in Scheme 4, and on spectroscopic evidence for the existence of **D** (see Experimental Section, compound **24**). Such an assumption is further supported (see below) by the isolation of intermediates in the reaction of **14** with $LiNMe_2$ (Scheme 6). The vinylidene functionality is a quite good spectroscopic probe, thus the stepwise conversion of **16** into **22** can be followed in the ^1H NMR spectrum. For **22**, the ^1H NMR spectrum revealed the presence of an equimolar mixture of the two possible geometrical isomers, with the two methyls cis or trans to each other. The spectrum, in fact, has

(23) (a) Hoffmann, R.; Lipscomb, W. N. *J. Chem. Phys.* **1962**, *36*, 2179. (b) Hoffmann, R. *J. Chem. Phys.* **1963**, *39*, 1397.

Scheme 6

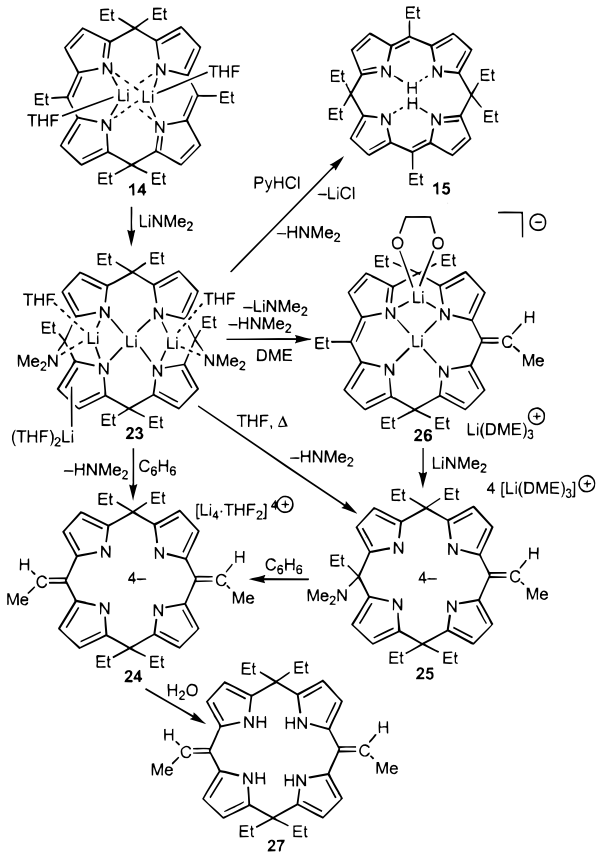

two quartets and two doublets of equal intensity for the vinylidene groups and eight doublets for the β-protons of the pyrroles. The simultaneous presence of the two possible isomers has been confirmed even in the solid state by the X-ray analysis, which reveals a statistical distribution of the Me and H groups around the vinylidene carbon in a ratio close to that observed in solution. An X-ray analysis was performed on crystals obtained from the recrystallization of **22** from DME. From this solvent the ion-separated form of **22** was obtained and the picture of the corresponding anion is reported in Figure 6.

The presence of two vinylidene substituents in the meso positions does not affect very much the overall conformation of the ligand, which displays the usual saddle-shaped form with a slight out-of-plane of the Ni ion (see Table 2). Both geometrical isomers, namely those having the two methyl groups C12 and C12′ cis or trans to each other, are present in the solid state in a ratio which is nearly the same as that in solution (1:1). The bonding sequence within the pyrrolyl anion is as expected, and the C10−C11 distance [1.32(1) Å] is in agreement with the presence of a double bond. Short Ni···H contacts [2.92 Å] from two *meso*-ethyl groups from the same side of the N_4 coordination plane were found. Although the ligand has two meso sp^2 carbon atoms, the ruffling around them is very high, thus minimizing the steric hindrance between the hydrogens of the pyrrolyl moieties and the CHMe groups.

Both **21** and **22** were obtained with good yield (>70%) in a multigram scale, and therefore the reactions reported (see the Experimental Section) can be used conveniently at the preparative level. The protonation of **21** and **22** (Scheme 6) leading to **16** reveals the nucleophilic reactivity of the vinylidene−porphyrinogen derivatives, a topic which will be discussed in the following. Complex **22** contains a novel form of porphyrinogen, which opens the synthetic access to a variety of

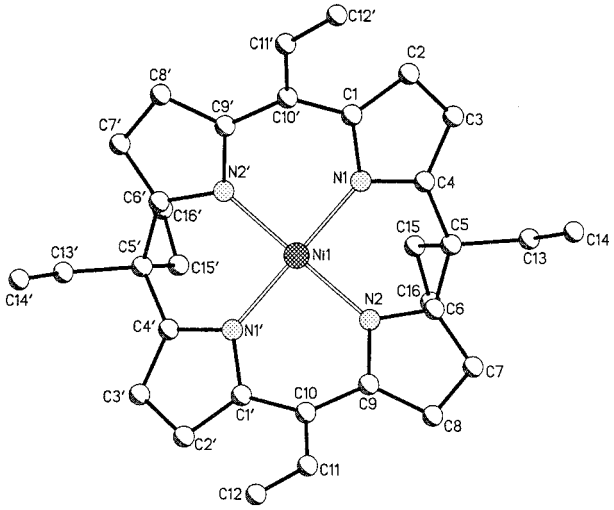

Figure 6. Ball-and-stick representation of the dianion of complex **22** showing the adopted labeling scheme [hydrogens, $Li(DME)_3^+$ cations and disorder omitted for clarity]. Prime denotes the following symmetry operation: $-x, y, -z + {}^1/_2$.

oxidized or functionalizable forms. The closest relationship we found for the bis-vinylidene−porphyrinogen is the 5,15-dioxoporphyrinogen reported several years ago and never structurally characterized.[24] The novel form of porphyrinogen in **22**, which may have considerable synthetic potential, can be available either from transmetalation or demetalation of **22**. We achieved, however, a much better synthetic approach to the bis-vinylidene−porphyrinogen tetraanion from the direct deprotonation of **14**. In addition, such a reaction shed light on the deprotonation mechanism of the porphodimethene skeleton as a function of the metal and the reaction solvent (Scheme 6). The addition of $LiNMe_2$ to **14** gave, regardless of the solvent used (THF, DME, benzene), the bisdimethylamino−porphyrinogen derivative **23**, which, upon heating, underwent $HNMe_2$ elimination to give different porphyrinogen derivatives, according to the solvent, namely **24** in benzene, **25** in THF, and **26** in DME. Scheme 6 displays also the relationship between **24**, **25**, and **26**. This relationship reveals the fundamental role of the reaction solvent. The complete elimination of $HNMe_2$ from **23** or **25** to form **24** occurs exclusively in a poorly coordinating solvent, which prevents from either **23** or **25** the loss of $LiNMe_2$ promoted by a polar solvent binding alkali cations. Thus, the thermal decomposition of **23** in THF, followed by the crystallization in DME, gave the elimination of a single $HNMe_2$ molecule and the formation of *meso*-vinylidene−dimethylamido derivative **25**, which undergoes the loss of a second $HNMe_2$ molecule to **24** exclusively in benzene. By running the reaction in DME, it has been shown how a coordinating solvent could affect the thermal evolution of **23**. In a preliminary step we isolated **26**, derived from the loss of $HNMe_2$ and $LiNMe_2$. Such a finding proves that the reaction of $LiNMe_2$ at the meso carbons of porphomethene or porphodimethene is reversible. Note that the addition of $LiNMe_2$ in DME at room temperature allowed the isolation of **25**. We mapped the entire transformation of the porphodimethene in vinylidene−porphyrinogen by analyzing the solid-state structure of complexes **23**−**26**. The structural investigation of the compounds displayed in Scheme 6 revealed three major characteristics: (*i*) the possible presence of geometrical isomers of **23** and **24**; (*ii*) the occurrence, as a function of the

(24) (a) Inhoffen, H. H.; Fuhrhop, J. H.; von der Haar, F. *Justus Liebig Ann. Chem.* **1966**, *700*, 92. (b) Fischer, H.; Treibs, A. *Justus Liebig Ann. Chem.* **1927**, *451*, 209.

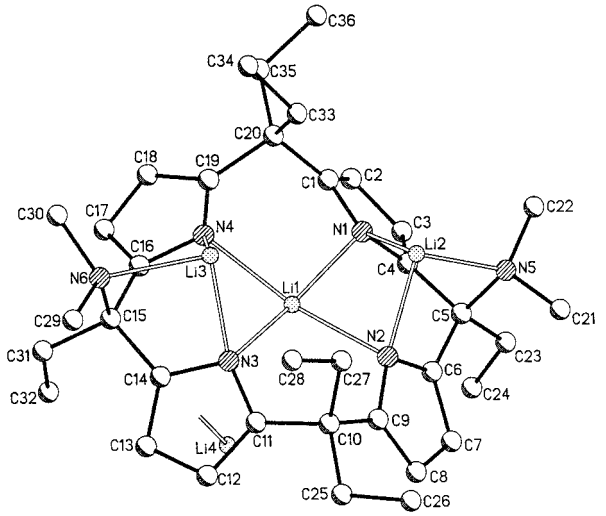

Figure 7. Ball-and-stick representation of complex **23** showing the adopted labeling scheme [hydrogens and solvent molecules omitted for clarity].

reaction or crystallization solvent, of an ion-pair or an ion-separated form for the same compound; and (*iii*) the solid state−solution structural relationship.

The latter aspect will be analyzed in detail comparing the structural information from the ^{1}H NMR spectra of **23** and **24** with their structures in the solid state. The structures of **24**, **25**, and **26** are available in the Supporting Information. The structure of **23** (Figure 7) differs considerably from that of **20**, which is also a doubly meso-functionalized porphyrinogen. The difference in the overall conformation is due to the presence of four lithium cations in the structure. The central cation has a distorted square pyramidal coordination, with an N_4 out-of-plane of −0.377(8) Å. Two adjacent pyrrole-nitrogen and one of the amino groups act as an N_3 tridentate ligand for the two lithium cations bonded to the periphery of the porphyrinogen, while the fourth lithium cation is η^5-bonded to one of the pyrrolyl anions. The lithium cations at the periphery force the syn arrangement of the dimethylamino groups. A selected list of the structural parameters is given in Table 3, whereas the conformational parameters are listed in Table 2. The ligand displays a dome conformation, and each lithium cation completes its coordination sphere with a THF molecule.

The three sets of signals for the ethyl groups in the ^{1}H NMR spectrum of **23** are in agreement with the presence of the syn isomer, which does not isomerize on standing in solution. Compound **24** is an equimolar mixture of the cis and trans isomers, as we found for the nickel derivative **22**, and this fact is supported by the equal intensity of the two quartets and the two doublets relative to the vinylidene groups. Coalescence of the two sets of signals was not observed even at high temperature. Compound **25** displays a C_1 symmetry in deuterated pyridine at room temperature. The possible rotation around the double bond was not observed on the NMR time scale at room temperature, as confirmed by the presence of eight doublets for the β hydrogens of the pyrroles in the spectrum. When the temperature of the deuterated pyridine or toluene solution of **25** was increased, its conversion into **26** and **24**, respectively, was observed. The ^{1}H NMR spectrum of **26**, with eight doublets for the β hydrogens of the pyrroles and two sets of dq for the *meso*-methylenes, supports the C_s symmetry, both at room and higher temperature.

Some major synthetic achievements reported in this section have to be emphasized: they are the formation of *meso*-

Scheme 7

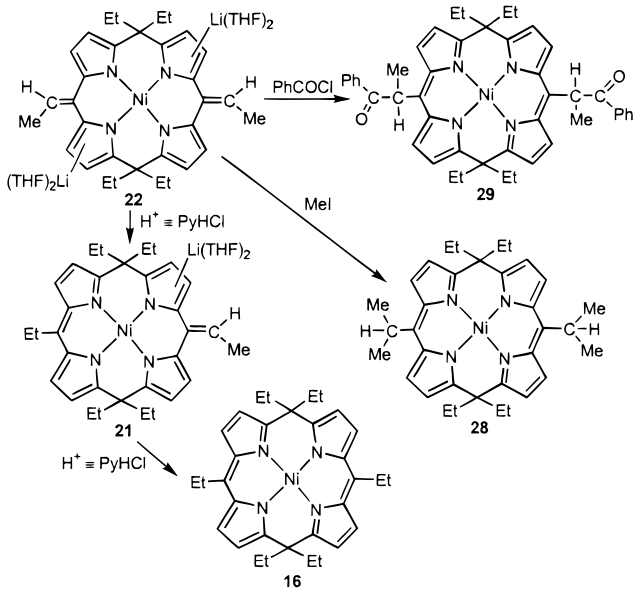

dimethylamino and *meso*-vinylidene porphyrinogens. The meso-functionalization and the formation of vinylidene derivatives can be performed equally well on transition metal, i.e. Ni(II), or alkali cation, i.e. Li, derivatives, the latter being much more suitable for any kind of metalation or protonation. The question at this stage concerns the possibility of converting the novel porphyrinogens to their protic form. The protonation of **23** is essentially occurring at the more basic sites, namely the diethylamino groups, thus causing the elimination of $HNMe_2$ and the formation of **15**. In contrast, under very controlled conditions, we were able to achieve the protonation of **24** with the formation of **27**. Following the procedure given in the Experimental Section, the selective protonation of the nitrogen occurred, without any protonation at the vinylidene functionality. The porphyrinogen **27** was isolated and fully characterized both in solution and in the solid state. A preliminary X-ray analysis supported the proposed structure.[19]

D. The Nucleophilic Reactivity of the Vinylidene−Porphyrinogen: The Meso-Functionalization of Porphodimethene. The reversible deprotonation−protonation sequence of the porphodimethene skeleton in Scheme 5 reveals the synthetic potentiality of the vinylidene−porphyrinogen derivatives. The reactions of **22** with the electrophiles listed in Scheme 7 give a glimmering of such a potentiality. The stepwise protonation of **22** using PyHCl led to **21**, then to **16**. The reaction of **22** with MeI parallels the protonation with the formation of the *meso*-bis-isopropyltetraethylporphodimethene−nickel, **28**. Such an unusual meso-substituted porphodimethene is hardly accessible from any other synthetic route. The reaction of **22** with PhCOCl shows how the introduction of a reactive functional group in the meso positions of porphodimethene can be achieved. The reaction led to the formation of the functionalized porphodimethene−Ni complex, **29**. The presence of two stereogenic centers in **29** reveals the possible use of **22** in the synthesis of chiral porphodimethenes.[19] Detailed characterization of **28** and **29** is discussed in the Experimental Section. The ^{1}H NMR spectra did not reveal any characteristics different from those of the other porphodimethenes so far reported.

Because of the synthetic relevance of the reaction of bis-vinylidene−porphyrinogens with electrophiles, a theoretical analysis on the electronic properties of the bis-vinylidene−porphyrinogen was carried out. The molecular orbitals of the

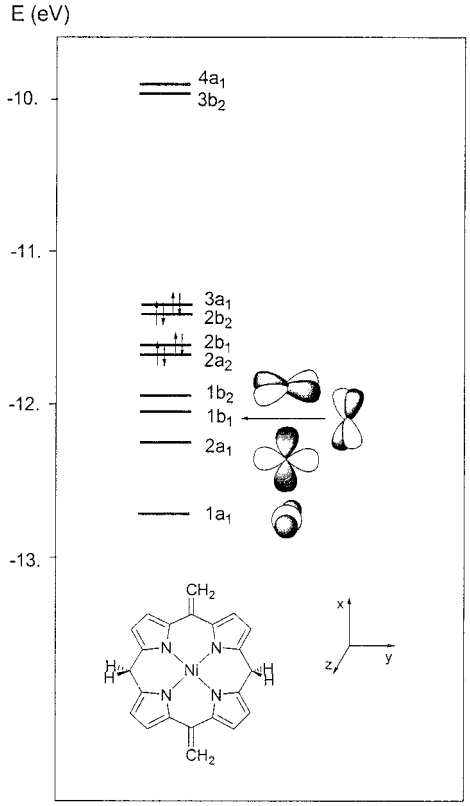

Figure 8. Molecular orbitals of the bis-vinylidene−porphyrinogen−nickel complex.

Chart 6

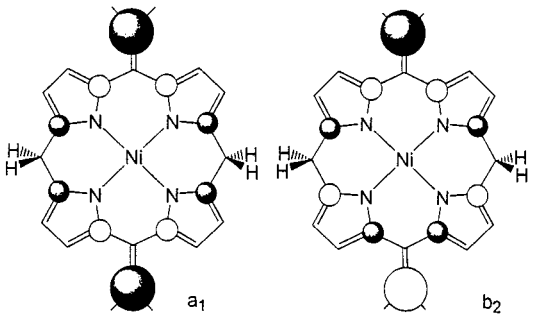

bis-vinylidene−porphyrinogen−nickel were built similarly to those of the nickel−porphodimethene fragment, and are displayed in Figure 8. The bis-vinylidene−porphyrinogen ligand was simplified by replacing the four ethyl groups on the meso carbons and the two methyl groups on the vinylidene unit with hydrogens. A comparison of Figures 5 and 8 shows that the modification from a hydrogen to a vinylidene group at the periphery of the model macrocyclic ligand affects neither the character nor the energy ordering of the metal orbitals. The main difference with the molecular orbital diagram of the porphodimethene complex consists of the presence of two high-lying occupied orbitals, $3a_1$ and $2b_2$, which are the HOMO and HOMO − 1 of the bis-vinylidene−porphyrinogen−Ni complex. These are ligand-centered orbitals mostly localized on the β-carbon atoms of the vinylidene groups (see Chart 6). It is therefore the presence of such orbitals that determines the observed regioselectivity of the electrophilic attack toward the vinylidene β-carbon atoms, which seems to be again frontier-orbital-controlled. An analysis of the gross atomic charges derived for the nickel bis-vinylidene−porphyrinogen show a significant negative charge on the vinylidene β-carbon atoms (−0.35) only slightly lower than for the nitrogen atoms (−0.51),

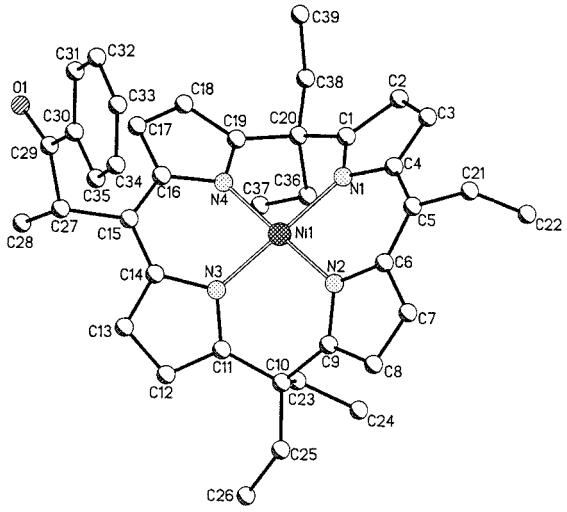

Figure 9. Ball-and-stick representation of complex **30** showing the adopted labeling scheme [hydrogens omitted for clarity].

Scheme 8

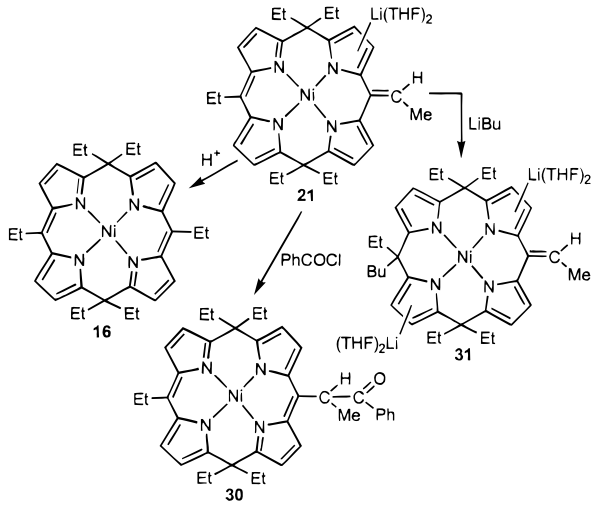

thus suggesting that the regioselectivity of the electrophilic attack could be directed by charge and orbital factors in concert. This agrees with the experimental evidence that the same regioselectivity is shown by both hard (H+) and soft (PhCOCl) electrophiles.

In the scenario so far presented on the meso-reactivity of the porphodimethene and bis-vinylidene−porphyrinogen, the chemistry of complex **21** deserves to be discussed and proved by a few examples such as those collected in Scheme 8. Complex **21** contains at the same time a nucleophilic and an electrophilic center in the meso-positions. Such a kind of bifunctionality is synthetically very attractive. The reaction with PhCOCl led to the monofunctionalized porphodimethene complex **30**, whereas the reaction with a nucleophile, i.e., LiBu, gave the nonsymmetric substituted porphyrinogen **31**. The structure of **30** is displayed in Figure 9. Complex **30** has structural features similar to those of complex **16**, nickel(II) being −0.046(3) Å out of the plane, while the ligand shows the usual saddle-shaped conformation. The metal is protected by the hydrogen from the methylenes of the *meso*-sp^3-ethyl groups (Ni1···H23B, 2.65; Ni1···H36B, 2.77). The dihedral angle between the phenyl ring and the $-CH-(C=O)-C_{Ph}$ fragment is 14.0(4)°. The torsion angles [O1−C29−C30−C31, −13(1)°; O1−C29−C30−C35, 166.6(7)°] give a picture of the orientation of the benzoyl substituent.

Scheme 9

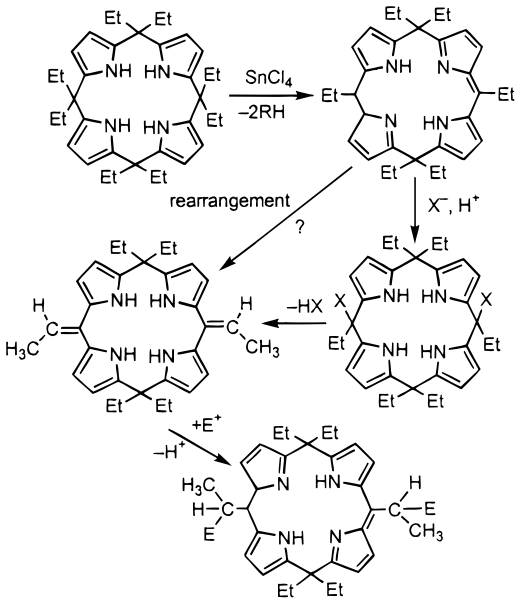

Conclusions

A novel synthetic methodology was established, which leads, through an unprecedented pathway, from porphyrinogen to porphomethene and porphodimethene. Such molecules, which were so far almost curiosities, become available in large quantities for synthetic and mechanistic purposes. Porphomethene and porphodimethene not only pave the way from porphyrinogen to porphyrins, but are the key for entering novel and functionalized forms of porphyrinogen. The electrophilic reactivity of the monosubstituted meso-positions of the porphodimethene leads to meso-functionalized porphyrinogens by the use of a large variety of nucleophiles. Among them, the dimethylamido anion causes the deprotonation of the *meso*-alkyl substituents, thus forming *meso*-vinylidene porphyrinogens. These latter compounds, very easily undergoing attack by electrophiles, generate functionalized porphodimethenes. The synthetic pathway from *meso*-octaalkylporphyrinogen to porphodimethene, functionalized porphyrinogen, and functionalized porphodimethene is depicted in Scheme 9.

Acknowledgment. We thank the "Fonds National Suisse de la Recherche Scientifique" (Bern, Switzerland, Grant No. 20-53336.98), Action COST D9 (European Program for Scientific Research, OFES No. C98.008), and Fondation Herbette (Université de Lausanne, N.R.) for financial support.

Supporting Information Available: ORTEP drawings (Figures S1−S7); details of the X-ray data collection, structure solution and refinement, tables giving crystal data and structure refinement, atomic coordinates, isotropic and anisotropic displacement parameters, and bond length and angles (Tables S1−S35) for **14**, **15**, **16**, **20**, **22**, **23**, and **30**. Crystal data (Tables S36−S60) and ball-and-stick drawings (Figures S8−S13) for **13**, **19**, **24**, **25**, and **26** (PDF). This material is available free of charge via the Internet at http://pubs.acs.org.

JA000253S